Initiation of a periodic array of cracks in the thermal shock problem: a gradient damage modeling

Paul Sicsic, Jean-Jacques Marigo, Corrado Maurini

Initiation of a periodic array of cracks in the thermal shock problem: a gradient damage modeling

Paul Sicsic[a,b,*], Jean-Jacques Marigo[a], Corrado Maurini[c,d]

[a] *Laboratoire de Mécanique des Solides (UMR-CNRS 7649), Ecole Polytechnique, 91128 Palaiseau Cedex*
[b] *Lafarge Centre de Recherche, 95 Rue de Montmurier 38290 St-Quentin-Fallavier, France*
[c] *Université Paris 6 (UPMC), 4 place Jussieu, 75252 Paris, France*
[d] *Institut Jean Le Rond d'Alembert (UMR-CNRS 7190), 4 place Jussieu, 75252 Paris, France*

Abstract

This paper studies the initiation of cracks in the thermal shock problem through the variational analysis of the quasi-static evolution of a gradient damage model. We consider a two-dimensional semi-infinite slab with an imposed temperature drop on its free surface. The damage model is formulated in the framework of the variational theory of rate-independent processes based on the principles of irreversibility, stability and energy balance. In the case of a sufficiently severe shock, we show that damage immediately occurs and that its evolution follows first a fundamental branch without localization. Then it bifurcates into another branch in which damage localization will take place to finally generate cracks. The determination of the time and mode of that bifurcation allows us to explain the periodic distribution of the so-initiated cracks and to calculate the crack spacing in terms of the material and loading parameters. Numerical investigations complete and quantify the analytical results.

Keywords: damage mechanics, gradient damage model, thermal shock, variational methods, energy balance, stability and bifurcation, Rayleigh ratio
2000 MSC: 74R10, 49J40, 26A45, 47J30

1. Introduction

The shrinkage of materials, induced by cooling or drying, may lead to arrays of regularly spaced cracks in a range of phenomena. Examples of such a situation come from various fields: civil engineering with the drying of concrete (Bisschop and Wittel, 2011), mechanical engineering with the exposure of glass (Geyer and Nemat-Nasser, 1982) or ceramics to a thermal shock (Bahr et al., 2010; Shao et al., 2010), geomaterials with the drying of soils (Morris et al., 1992; Chertkov, 2002; Goehring et al., 2009) or colloidal suspensions (Gauthier et al., 2010), and the thermal shocks in overexploited gas storage caverns (Berest et al., 2012). These cracks are of importance as they can weaken the body or govern future diffusion process, modify the strength of the material (Shao et al., 2011) or compromise the safety of the structure.

In this paper, we focus on the thermal shock problem of a brittle slab, for which experimental results are reported in Bahr et al. (1986), Shao et al. (2010), and Geyer and Nemat-Nasser (1982). The specimen is a thin slab, free at the boundary, composed of a homogeneous material without prestress in its initial configuration. It is uniformly heated and then quenched in a cold bath inducing a thermal shock on the exposed surfaces. Figure 1 reports an example of the observed crack pattern at the end of the cooling process (from Jiang et al., 2012). The central part of the specimen, where the temperature field only depends on the distance from the wet surface, presents an array of parallel cracks. Some of these cracks stop earlier during the penetration and the spacing of the crack increases with the depth.

*Corresponding author: paul.sicsic@polytechnique.edu

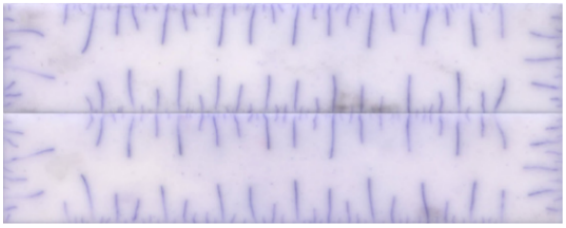

Figure 1: Crack pattern on both faces of a thin slab (1mm × 10mm × 50mm) after a thermal shock (from Jiang et al., 2012)

The theoretical and numerical aspects of multiple cracking under thermal shock have been studied by many authors using classical tools of the Griffith theory of fracture mechanics (Hasselman, 1969; Lu and Fleck, 1998; Bazant et al., 1979; Bahr et al., 1988; Jagla, 2002; Jenkins, 2005; Bahr et al., 2010; Jiang et al., 2012). The most intriguing phenomena are the period doubling in the crack spacing during the propagation inside the body and the crack initiation. The existing studies assume *a priori* that the cracks are straight, parallel to each other, and periodically distributed. Hence, they usually perform energetic analyses based on numerical or semi-analytical calculations of the strain energy associated to uniform or alternate crack propagation modes. In this context, Bazant et al. (1979) explain selective crack arrest using a bifurcation analysis based on the change of sign of the second derivative of the strain energy with respect to the crack penetration. Bahr et al. (1988) perform a similar analysis with numerical boundary element calculations and discuss crack initiation assuming periodicity and the presence of initial flaws. Jagla (2002) discusses the initiation and propagation of the periodic crack pattern using a stress criterion for initiation and energy minimality for optimal spacing. More recently, Jenkins (2005) and Jiang et al. (2012) study spacing and initiation by global minimization of the Griffith energy. Bahr et al. (2010) derives semi-analytical scale laws for the spacing of the cracks as a function of the penetration and the severity of the thermal shock.

Removing the hypothesis on the topology of the crack pattern remains a major issue within classical fracture mechanics. Yet similar problems may be naturally tackled, theoretically and numerically, in the framework of the variational approach to fracture mechanics proposed by Francfort and Marigo (1998). This approach, now well established, extends the energetic theory of Griffith by treating the crack geometry as a genuine unknown. It is based on the minimization of the sum of the elastic energy and the crack energy among all admissible crack states. The associated numerical solution strategy proposed by Bourdin et al. (2000) relies on a regularized functional approximating the total Griffith energy in the sense of Gamma-convergence (Ambrosio, 1990; Braides, 2002). The regularized formulation introduces a smeared representation of the crack through a smooth scalar field, which may be mechanically interpreted as a damage variable. The corresponding total energy may be assimilated with that of a non-local gradient damage model in the framework of the general theory developed in Pham and Marigo (2010a,b). The link between the damage model quantities and those of the Griffith theory have been extensively studied on a theoretical and numerical view-point in the one-dimensional case (Pham and Marigo, 2013). Similar numerical methods become nowadays quite popular in the community of applied numerical engineering (Miehe et al., 2010; Borden et al., 2012).

For the thermal shock problem of Figure 1, Bourdin et al. (2011) report preliminary numerical results obtained through the variational approach, focusing on the spacing between cracks as a function of the depth. We use similar numerical simulations for an illustration of the phenomenology at initiation. The reader is referred to (Bourdin, 2007) for the details about the numerical implementation. Figure 2 reports the evolution of a scalar damage field α, affecting the stiffness of the material and varying between 0 (sound material) and 1 (totally damaged material). Cracks are represented as bands, of finite width, with localized damage (in red in the figure). If the loading is not large enough, the solution remains elastic and no damage is observed. For sufficiently severe thermal shocks, a careful numerical computation (Fig. 2) shows the following main stages:

1. Starting at $t = 0$ and for small times, a strip with diffuse damage propagates inside the body. Damage decreases from a maximal value at the surface towards zero, being homogeneous in the direction parallel

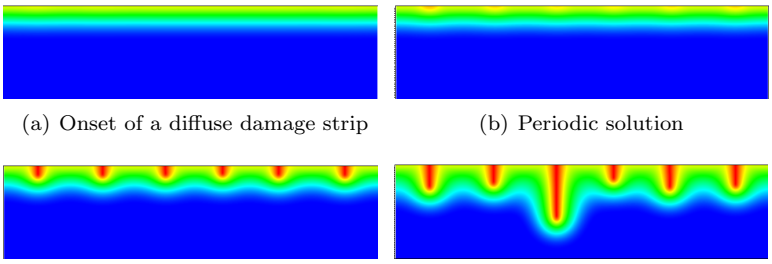

(a) Onset of a diffuse damage strip (b) Periodic solution

(c) Array of fully developed of cracks (d) Selecting crack arrest

Figure 2: Damage variable α for four time steps of the minimization process. The loading is given by the thermal shrinking induced by cooling through the top surface. In blue, the sound material; in red, the totally damaged material.

to the surface of the thermal shock.

2. At some critical time t_b, the homogeneous solution bifurcates towards a solution including a set of periodically distributed damaged bands penetrating inside the body.
3. The damage field grows until 1 (fully damaged material) in the mid-line of these zones. A set of periodically distributed cracks of equal length has formed and starts propagating inside the body.
4. Some damage bands stop to propagate whereas the other ones continue penetrating inside the body.

This numerical behavior is a typical illustration of the strength of the variational approach to fracture. Indeed, after a diffuse damaging phase (step 1), it captures crack initiation (steps 2-3), as well as crack propagation (step 4). This paper focuses on the steps (1)-(2), attempting to analytically justify and quantitatively predict the results of these numerical experiments in the framework of the variational theory of gradient damage models (Pham and Marigo, 2010a,b). Differently from previous works on thermal shocks, where initiation is obtained by introducing initial flows or assuming the topology of the crack pattern, here we start with a truly sound and uniform material.

The aim of this paper is two-fold: (i) give further insight on the initiation phenomenon in thermal shock fracture, and, more generally, on the morphogenesis of complex crack patterns; (ii) provide a non-trivial example of the study of the evolution and bifurcation problem of gradient damage models in a two dimensional settings. We focus on the thermal shock problem for a semi-infinite two-dimensional slab, in a quasi-static setting. By assuming a perfect conductivity at the surface of the thermal shock, we impose a Dirichlet boundary condition on the temperature and use the analytically calculated temperature field, function of space and time, to evaluate the mechanical loading in the form of thermally induced inelastic strains. We consider the same damage model used in the regularized approach of the numerical simulations of Figure 2. This model fits into the family of models introduced in (Pham and Marigo, 2010a,b), for which a general analysis of the one-dimensional traction problem has been reported in (Pham et al., 2011; Pham and Marigo, 2013). It is characterized by a scalar damage variable and a gradient term in the damage for the regularization, which introduces an internal length ℓ. The corresponding quasi-static evolution problem is formulated in the framework of the variational theory of rate-independent processes, imposing the three requirements of stability, irreversibility, and energy balance (Propositions 2). The loading is controlled by the thermal shock mildness parameter $\theta = \sigma_{\mathsf{c}}/(\mathsf{E}\,\mathsf{a}\vartheta)$, where σ_{c} is the critical stress of the material, ϑ the temperature drop at the surface, a the thermal expansion coefficient and E the Young modulus. For mild shocks ($\theta \geq 1$), one trivially obtains that the solution remains purely elastic and the damage is null at any time. For sufficiently severe shock ($\theta < 1$), the damage criterion is reached at the beginning of the evolution. Looking for a solution invariant in the direction x_1 parallel to the surface of thermal shock, we show the existence of a fundamental solution with diffused damage localized in a finite strip (Proposition 3), where the damage field monotonically decreases from a maximum value at the surface to zero at a finite depth D_t^* (as in Figure 2(a)). Hence, we formulate the rate problem (Proposition 5) and the second-order stability conditions (Proposition 1) about this fundamental solution, whose uniqueness and stability are determined through the minimization of a Rayleigh ratio on linear spaces or convex cones (Proposition 8). The main result of this paper is the solution of this bifurcation and stability problem (Proposition 10),

which is obtained by adopting a partial Fourier decomposition in the direction parallel to the surface of the slab. We prove the existence of a finite time t_b from which a bifurcation from the fundamental branch can occur, the fundamental branch becoming unstable at a later time t_s. Moreover we show that the bifurcated solution is stable (Proposition 7) and characterized by a finite wavelength λ_b proportional to the internal length ℓ of the material. This bifurcated solution represents the onset of the localization phenomena leading to the establishment of the periodic crack pattern observed in the experiments. Quantitative results are obtained through the numerical solution of a one-dimensional boundary value problem for the fundamental branch and of a parametric one-dimensional eigenvalue problem for establishing the key properties of the bifurcated solution as a function of the loading parameter θ and the Poisson ratio.

Specifically the paper is organized as follows. Section 2 formalizes the thermal shock problem in a two dimensional setting and recalls the formulation of the gradient damage model. Section 3 establishes the fundamental solution in the elastic and damaged case. The following section is devoted to the bifurcation and loss of stability of this fundamental branch. In Section 4.1 we formalize the rate problem, then we characterize bifurcation and stability by Rayleigh's ratio minimization (Section 4.2) and give the main properties of the Rayleigh ratio (Section 4.3). We then characterize the first bifurcation (Section 4.4). The numerical computation are gathered in Section 5, dealing first with the fundamental solution and then with the bifurcation problem. The key results are resumed and commented in Section 6. Section 7 draws conclusions and suggests future extensions.

Nomenclature and notation. A list of the main symbols and notations adopted in the paper is reported in Table 1. The summation convention on repeated indices is implicitly adopted. The vectors and second order tensors are indicated by boldface letters, like $\mathbf{u}$ and $\boldsymbol{\sigma}$ for the displacement field and the stress field. Their components are denoted by italic letters, like u_i and σ_{ij}. The fourth order tensors as well as their components are indicated by a boldface letters, like $\mathbf{A}$ or $\mathbf{A}_{ijkl}$ for the stiffness tensor. Such tensors are considered as linear maps applying on vectors or second order tensors and the application is denoted without dots, like $\mathbf{A}\boldsymbol{\varepsilon}$ whose ij-component is $\mathbf{A}_{ijkl}\varepsilon_{kl}$. The inner product between two vectors or two tensors of the same order is indicated by a dot, like $\mathbf{a}\cdot\mathbf{b}$ which stands for a_ib_i or $\boldsymbol{\sigma}\cdot\boldsymbol{\varepsilon}$ for $\sigma_{ij}\varepsilon_{ij}$. The symbol $\otimes$ denotes the tensor product and $\otimes_s$ its symmetrized, *i.e.* $2\mathbf{e}_1\otimes_s\mathbf{e}_2=\mathbf{e}_1\otimes\mathbf{e}_2+\mathbf{e}_2\otimes\mathbf{e}_1$. $\mathbb{M}_s$ denotes the space of 2×2 symmetric tensor and $\mathbf{I}$ is its identity tensor. The classical convention is adopted for the orders of magnitude: $o(\epsilon)$ denotes functions of ϵ such that $\lim_{\epsilon\to 0} o(\epsilon)/\epsilon = 0$. If $\mathcal{A}(\cdot)$ represents a quadratic form defined on a Hilbert space, the associated symmetric bilinear form is denoted by $\mathcal{A}\langle\cdot,\cdot\rangle$, *i.e.*

$$4\mathcal{A}\langle\boldsymbol{\chi},\boldsymbol{\xi}\rangle := \mathcal{A}(\boldsymbol{\chi}+\boldsymbol{\xi}) - \mathcal{A}(\boldsymbol{\chi}-\boldsymbol{\xi}).$$

2. Setting of the problem and damage law

2.1. Setting of the gradient damage model

We simply recall here the main steps of the construction of a gradient damage model by a variational approach, the reader interested by more details should refer to Pham and Marigo (2010a,b). Since the application will concern a very thin body, we describe the behavior in a plane stress setting corresponding to the membrane theory of plates (without bending). Thus we consider a homogeneous (two-dimensional) plate made of a damaging isotropic material whose behavior is defined as follows:

1. The damage parameter is a scalar which can only grow from 0 to 1, $\alpha = 0$ denoting the undamaged state and $\alpha = 1$ the completely damaged state.
2. The state of the volume element is characterized by the triplet $(\boldsymbol{\varepsilon}^e, \alpha, \mathbf{g})$ where $\boldsymbol{\varepsilon}^e$, α and $\mathbf{g}$ denote respectively the elastic (in-plane) strain tensor, the damage parameter and the gradient of damage vector ($\mathbf{g} = \nabla\alpha$).
3. The bulk energy density of the material is the state function $W : (\boldsymbol{\varepsilon}^e, \alpha, \mathbf{g}) \mapsto W(\boldsymbol{\varepsilon}^e, \alpha, \mathbf{g})$. Therefore, the material behavior is *non local* in the sense that it depends on the gradient of damage. We assume

Material and geometric constants	
E, ν	Young modulus and Poisson ratio (sound material)
a, $\mathsf{k_c}$	Thermal expansion and thermal diffusivity
σ_c, ℓ	Critical stress (10) and internal length of the damage model
L	Width of the slab (Fig. 2.2)
Space and time variables	
$\mathbf{x} = (x_1, x_2)$	Space variables in the physical space
t	Physical time variable
$y = x_2/2\sqrt{\mathsf{k_c}t}$	Rescaled depth variable adapted to the diffusion process
$\tau = 2\sqrt{\mathsf{k_c}t}/\theta\ell$	Rescaled time adapted to the fundamental solution (35)
Thermal Loading	
ϑ	Temperature drop at the surface
$\mathsf{f_c}$	Complementary error function (Fig. 2.2)
$\theta = \sigma_\mathsf{c}/\mathsf{a}\vartheta\mathsf{E}$	Thermal shock mildness parameter (34)
$\boldsymbol{\varepsilon}_t^{\rm th}(\mathbf{x})$	Thermal strain field (14)
$\boldsymbol{\varepsilon}_t(\mathbf{x})$	Total strain field
$\boldsymbol{\varepsilon}_t^e(\mathbf{x}) = \boldsymbol{\varepsilon}_t(\mathbf{x}) - \boldsymbol{\varepsilon}_t^{\rm th}(\mathbf{x})$	Elastic strain field (14)
Fundamental Branch	
$\alpha_t^*(\mathbf{x}),\ \mathbf{u}_t^*(\mathbf{x}),\ \boldsymbol{\sigma}_t^*(\mathbf{x})$	Damage, displacement and stress fields in the physical variables $t, \mathbf{x}$
$\boldsymbol{\chi}_t^* = (\mathbf{u}_t^*, \alpha_t^*)$	state fields vector
$\bar\alpha_\tau(y), \bar{\boldsymbol{\sigma}}_\tau(y)$	Damage and stress field in the scaled variables τ, y
D_t^*	Damage penetration in the physical variables $t, \mathbf{x}$
$\delta_\tau = D_t^*/2\sqrt{\mathsf{k_c}t}$	Damage penetration in the scaled variables τ, y (35)
Bifurcation and Stability	
$\zeta = x_2/\mathsf{D}_t^*$	Rescaled depth variable adapted to the damage penetration (57)
$\mathcal{R}_t^*(\mathbf{v}, \beta)$	Rayleigh Ratio (53) studying the positivity of $\mathcal{E}_t''(\boldsymbol{\chi}_t^*)$
R_t^b	Minimum value of the Rayleigh ratio $\mathcal{R}_t^*(\mathbf{v}, \beta)$ over $\mathcal{C}\times\dot{\mathcal{D}}_t$ (54) and of $\bar{\mathcal{R}}_\tau^\kappa(\mathbf{V}, \beta)$ over $\mathbb{R}^+ \times \mathbf{H} \times \mathcal{H}_0$ (60)
R_t^s	Minimum value of the Rayleigh ratio $\mathcal{R}_t^*(\mathbf{v}, \beta)$ over $\mathcal{C}\times\dot{\mathcal{D}}_t^+$ (55)
t_b, t_s	First time of bifurcation and loss of stability (65)
$\mathbf{v}^b, \beta^b$	Mode of bifurcation (66)–(67)
k, κ	Wave number corresponding to the periodic solution (57)–(58)
$(\kappa_b, \hat{\mathbf{V}}^b, \hat\beta^b)$	Normalized minimizers of $\bar{\mathcal{R}}_{\tau_b}^\kappa(\mathbf{V}, \beta)$
$\tau_b,\ \delta_{\tau_b}$	Rescaled time and damage penetration associated to the first bifurcation time
$\lambda_b = 2\pi\theta\delta_{\tau_b}\tau_b\ell/\kappa_b$	Wavelength of the first bifurcation solution (68)
$\mathsf{D}_b = 2\delta_{\tau_b}\sqrt{\mathsf{k_c}t_b} = \theta\delta_{\tau_b}\tau_b\ell$	Damage penetration at the first bifurcation point (69)

Table 1: Main nomenclature

that the bulk energy density is the sum of three terms: the stored elastic energy $\psi(\boldsymbol{\varepsilon}^e, \alpha)$, the local part of the dissipated energy by damage $w(\alpha)$ and its non local part $\frac{1}{2}\mathsf{w}\ell^2\mathbf{g}\cdot\mathbf{g}$,

$$W(\boldsymbol{\varepsilon}^e, \alpha, \mathbf{g}) = \psi(\boldsymbol{\varepsilon}^e, \alpha) + w(\alpha) + \frac{1}{2}\mathsf{w}\ell^2\mathbf{g}\cdot\mathbf{g}, \tag{1}$$

each of these terms enjoying the following properties:

(a) The elastic energy reads as

$$\psi(\boldsymbol{\varepsilon}^e, \alpha) = \frac{1}{2}(1-\alpha)^2\mathbf{A}\boldsymbol{\varepsilon}^e\cdot\boldsymbol{\varepsilon}^e, \tag{2}$$

where $\mathbf{A}$ is the stiffness tensor of the sound material. Thus, $(1-\alpha)^2\mathbf{A}$ represents the stiffness tensor of the material in the damage state α, it decreases from $\mathbf{A}$ to $\mathsf{0}$ when α grows from 0 to 1. The material being isotropic and by virtue of the plane stress assumption, the in-plane stiffness coefficients read as

$$\mathbf{A}_{ijkl} = \frac{\nu\mathsf{E}}{1-\nu^2}\delta_{ij}\delta_{kl} + \frac{\mathsf{E}}{2(1+\nu)}(\delta_{ik}\delta_{jl}+\delta_{il}\delta_{jk}), \qquad i,j,k,l\in\{1,2\}, \tag{3}$$

where E represents the Young modulus of the sound material and ν is the Poisson ratio (which does not change throughout the damage process). The compliance tensor of the sound material will be denoted by S. Hence $\mathsf{S} = \mathbf{A}^{-1}$ reads as

$$\mathsf{S}_{ijkl} = -\frac{\nu}{\mathsf{E}}\delta_{ij}\delta_{kl} + \frac{1+\nu}{2\mathsf{E}}(\delta_{ik}\delta_{jl}+\delta_{il}\delta_{jk}), \qquad i,j,k,l\in\{1,2\}. \tag{4}$$

(b) The local dissipated energy density reads as

$$w(\alpha) = \mathsf{w}\alpha \tag{5}$$

and hence is a positive increasing function of α, increasing from 0 when $\alpha = 0$ to the finite positive value w when $\alpha = 1$. Therefore w represents the energy dissipated during a complete, homogeneous damage process of a volume element: $\mathsf{w} = w(1)$.

(c) The non local dissipated energy density is assumed to be a quadratic function of the gradient of damage. Since the damage parameter is dimensionless and by virtue of the above definition of w, ℓ has the dimension of a length. Accordingly, ℓ can be considered as an internal length characteristic of the material while having always in mind that the definition of ℓ depends on the normalizations associated with the choices of the critical value 1 for α and w for the multiplicative factor.

4. The dual quantities associated with the state variables are respectively the stress tensor $\boldsymbol{\sigma}$, the energy release rate density Y and the damage flux vector $\mathbf{q}$:

$$\boldsymbol{\sigma} = \frac{\partial W}{\partial \boldsymbol{\varepsilon}^e}(\boldsymbol{\varepsilon}^e, \alpha, \mathbf{g}), \qquad \mathsf{Y} = -\frac{\partial W}{\partial \alpha}(\boldsymbol{\varepsilon}^e, \alpha, \mathbf{g}), \qquad \mathbf{q} = \frac{\partial W}{\partial \mathbf{g}}(\boldsymbol{\varepsilon}^e, \alpha, \mathbf{g}). \tag{6}$$

Accordingly, these dual quantities are given by the following functions of state:

$$\boldsymbol{\sigma} = (1-\alpha)^2\mathbf{A}\boldsymbol{\varepsilon}^e, \qquad \mathsf{Y} = (1-\alpha)\mathbf{A}\boldsymbol{\varepsilon}^e\cdot\boldsymbol{\varepsilon}^e - \mathsf{w}, \qquad \mathbf{q} = \mathsf{w}\ell^2\mathbf{g}. \tag{7}$$

The underlying *local* behavior is characterized by the function W_0 defined by $W_0(\boldsymbol{\varepsilon}^e, \alpha) = W(\boldsymbol{\varepsilon}^e, \alpha, \mathbf{0})$. This corresponds to a strongly brittle material, in the sense of (Pham and Marigo, 2013, Hypothesis 1), *i.e.* the material has a softening behavior and the energy dissipated during a process where the damage parameter grows from 0 to 1 is finite. The latter property is ensured by the fact that $w(1) < +\infty$. The former one requires that the elastic domain in the strain space $\mathcal{R}(\alpha)$ is an increasing function of α while the elastic domain in the stress space $\mathcal{R}^*(\alpha)$ is a decreasing function of α. Those elastic domains are defined by

$$\mathcal{R}(\alpha) = \left\{\boldsymbol{\varepsilon}^e\in\mathbb{M}_s \ : \ \frac{\partial W_0}{\partial\alpha}(\boldsymbol{\varepsilon}^e,\alpha)\geq 0\right\}, \qquad \mathcal{R}^*(\alpha) = \left\{\boldsymbol{\sigma}\in\mathbb{M}_s \ : \ \frac{\partial W_0^*}{\partial\alpha}(\boldsymbol{\sigma},\alpha)\leq 0\right\}$$

where $W_0^*(\boldsymbol{\sigma},\alpha) = \sup_{\boldsymbol{\varepsilon}\in\mathbb{M}_s}\{\boldsymbol{\sigma}\cdot\boldsymbol{\varepsilon}^e - W_0(\boldsymbol{\varepsilon}^e,\alpha)\}$ and $\mathbb{M}_s$ denotes the space of symmetric 2×2 tensors.

In the present context, one gets

$$W_0(\boldsymbol{\varepsilon}^e,\alpha) = \frac{1}{2}(1-\alpha)^2\mathbf{A}\boldsymbol{\varepsilon}^e\cdot\boldsymbol{\varepsilon}^e + \mathsf{w}\alpha \tag{8}$$

and hence

$$W_0^*(\boldsymbol{\sigma},\alpha) = \boldsymbol{\sigma}\cdot\boldsymbol{\varepsilon}^0 + \frac{1}{2(1-\alpha)^2}\mathsf{S}\boldsymbol{\sigma}\cdot\boldsymbol{\sigma} - \mathsf{w}\alpha. \tag{9}$$

Accordingly, the elastic domains $\mathcal{R}(\alpha)$ and $\mathcal{R}^*(\alpha)$ now read

$$\mathcal{R}(\alpha) = \{\boldsymbol{\varepsilon}^e\in\mathbb{M}_s\,:\,\mathbf{A}\boldsymbol{\varepsilon}^e\cdot\boldsymbol{\varepsilon}^e \le \frac{\mathsf{w}}{1-\alpha}\},\qquad \mathcal{R}^*(\alpha) = \{\boldsymbol{\sigma}\in\mathbb{M}_s\,:\,\mathsf{S}\boldsymbol{\sigma}\cdot\boldsymbol{\sigma}\le(1-\alpha)^3\mathsf{w}\}$$

and one immediately checks that the softening properties are satisfied. The critical stress σ_c (which represents for this specific damage model both the yield stress and the peak stress) in a uniaxial tensile test such that $\boldsymbol{\sigma} = \sigma_c\mathbf{e}_1\otimes\mathbf{e}_1$ is then given by

$$\sigma_c = \sqrt{\mathsf{w}\mathsf{E}}. \tag{10}$$

2.2. The body and its thermal loading

The natural reference configuration of the plate (Figure 2.2) is the semi-infinite strip $\Omega = (0,+\mathsf{L})\times(0,+\infty)$. We assume that the length L is much greater than the internal length ℓ of the material. (This assumption plays a role in the bifurcation and stability analyses - Section 4.) The body forces are neglected. The sides $x_1 = 0$ or L are submitted to boundary conditions so that the normal displacement and the shear stress vanish, whereas the side $x_2 = 0$ is free. Accordingly, the mechanical boundary conditions read as

$$u_1|_{x_1=0 \text{ or } \mathsf{L}} = 0,\quad \sigma_{21}|_{x_1=0 \text{ or } \mathsf{L}} = 0, \tag{11}$$

$$\sigma_{22}|_{x_2=0} = \sigma_{12}|_{x_2=0} = 0. \tag{12}$$

In $x_1 = 0$ or L and $x_2 = 0$ no boundary condition are imposed on the damage field, which can thus freely evolve. Up to time 0, the plate is at the reference uniform temperature T_0 and hence in its reference configuration, stress free and undamaged:

$$\mathbf{u}_t(\mathbf{x}) = \mathbf{0},\quad \boldsymbol{\varepsilon}_t^e(\mathbf{x}) = \mathbf{0},\quad \alpha_t(\mathbf{x}) = 0,\quad \boldsymbol{\sigma}_t(\mathbf{x}) = \mathbf{0},\quad \forall\mathbf{x}\in\Omega,\quad \forall t\le 0.$$

From time 0, a colder temperature $T_1 = T_0 - \vartheta$ is prescribed on the side $x_2 = 0$. Assuming that the temperature field is not influenced by the damage evolution and that the sides $x_1 = 0$ or L are thermally insulated, the diffusion of the temperature inside the body is governed by the classical heat equation. Therefore, assuming the temperature boundary condition in $x_2 = 0$ is of Dirichlet type, the temperature field at time $t > 0$ is given by

$$T_t(\mathbf{x}) = T_0 - \vartheta\,\mathsf{f_c}\Big(\frac{x_2}{2\sqrt{\mathsf{k_c}t}}\Big),\quad \forall t>0, \tag{13}$$

where $\mathsf{f_c}$ it the complementary error function (Figure 2.2), strictly decreasing from 1 to 0 at infinity, *i.e.*

$$\mathsf{f_c}(x) = \frac{2}{\sqrt{\pi}}\int_x^\infty e^{-s^2}\,\mathrm{d}s,$$

and $\mathsf{k_c}$ is the thermal diffusivity, a material constant. Thus the temperature field is uniform with respect to the x_1 direction.

At every time t, the elastic strain field $\boldsymbol{\varepsilon}_t^e$ is the difference between the total strain field $\boldsymbol{\varepsilon}_t$ and the thermal strain field $\boldsymbol{\varepsilon}_t^{\mathrm{th}}$. Since the material is isotropic, assuming that the shrinkage is linear, this latter one reads as $\boldsymbol{\varepsilon}_t^{\mathrm{th}}(\mathbf{x}) = \mathsf{a}(T_t(\mathbf{x}) - T_0)\mathbf{I}$, where a denotes the thermal dilatation coefficient of the material and $\mathbf{I}$ is the identity tensor of $\mathbb{M}_s$. Accordingly, the thermal and elastic strain fields read as

$$\boldsymbol{\varepsilon}_t^{\mathrm{th}}(\mathbf{x}) = -\mathsf{a}\vartheta\,\mathsf{f_c}\Big(\frac{x_2}{2\sqrt{\mathsf{k_c}t}}\Big)\mathbf{I},\qquad \boldsymbol{\varepsilon}_t^e(\mathbf{x}) = \boldsymbol{\varepsilon}(\mathbf{u}_t)(\mathbf{x}) + \mathsf{a}\vartheta\,\mathsf{f_c}\Big(\frac{x_2}{2\sqrt{\mathsf{k_c}t}}\Big)\mathbf{I}, \tag{14}$$

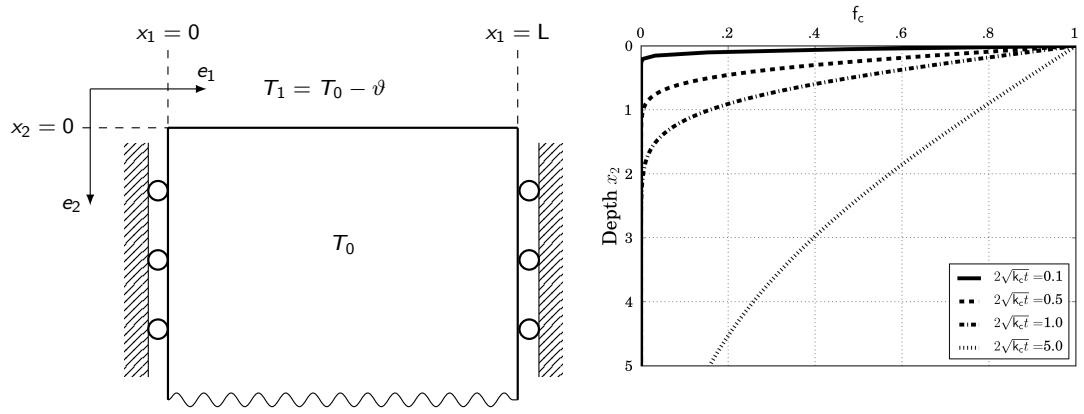

(a) Mechanical and thermal boundary conditions.

(b) The complementary error function.

Figure 3: Thermal shock problem statement.

where $\boldsymbol{\varepsilon}(\mathbf{u}_t)$ is the symmetrized part of the gradient of $\mathbf{u}_t$. The loading (14) induces positive shrinkage without positive stress. This justifies the use of a damage model that does not differentiate the effect of compression and traction.

We will only consider the first stage of the damage process so that α reaches nowhere the critical value 1 corresponding to the loss of rigidity of the material. Accordingly, the set of admissible damage fields $\mathcal{D}$ and the set of kinematically admissible displacement fields $\mathcal{C}$ are defined as

$$\mathcal{D} := \{\beta \in H^1(\Omega) \,:\, 0 \le \beta < 1 \text{ in } \Omega\}, \qquad \mathcal{C} := \{\mathbf{v} \in H^1(\Omega)^2 \,:\, v_1 = 0 \text{ on } x_1 = 0 \text{ or } \mathsf{L}\} \tag{15}$$

where $H^1(\Omega)$ denotes the usual Sobolev space of functions which are square integrable over Ω and whose distributional gradient is also square integrable. The spaces $\mathcal{D}$ and $\mathcal{C}$ are time independent and are equipped with the natural norm of $H^1(\Omega)$. With every pair of admissible displacement and damage fields, *i.e.* with every $(\mathbf{v}, \beta) \in \mathcal{C} \times \mathcal{D}$, one associates the total energy of the body at time t in this state, that is

$$\begin{aligned} \mathcal{E}_t(\mathbf{v}, \beta) &:= \int_\Omega W(\boldsymbol{\varepsilon}(\mathbf{v}) - \boldsymbol{\varepsilon}_t^{\mathrm{th}}, \beta, \nabla\beta)\, \mathrm{d}\mathbf{x} \\ &= \int_\Omega \Big(\frac{1}{2}(1-\beta)^2 \mathbf{A}(\boldsymbol{\varepsilon}(\mathbf{v}) - \boldsymbol{\varepsilon}_t^{\mathrm{th}}) \cdot (\boldsymbol{\varepsilon}(\mathbf{v}) - \boldsymbol{\varepsilon}_t^{\mathrm{th}}) + \mathsf{w}\beta + \frac{\mathsf{w}\ell^2}{2} \nabla\beta \cdot \nabla\beta \Big)\, \mathrm{d}\mathbf{x}. \end{aligned} \tag{16}$$

where $\boldsymbol{\varepsilon}(\mathbf{v})$ denotes the symmetrized gradient of $\mathbf{v}$.

Throughout the paper we use the directional derivatives of $\mathcal{E}_t$ and its partial derivatives with respect to time. All these derivatives up to the second order are defined below.

Definition 1 (Derivatives of the total energy)**.**

1. *First partial derivative with respect to t:*

$$\dot{\mathcal{E}}_t(\mathbf{v}, \beta) = -\int_\Omega (1-\beta)^2 \mathbf{A}(\boldsymbol{\varepsilon}(\mathbf{v}) - \boldsymbol{\varepsilon}_t^{\mathrm{th}}) \cdot \dot{\boldsymbol{\varepsilon}}_t^{\mathrm{th}}\, \mathrm{d}\mathbf{x}; \tag{17}$$

2. *Second partial derivative with respect to t:*

$$\ddot{\mathcal{E}}_t(\mathbf{v}, \beta) = \int_\Omega \Big((1-\beta)^2 \mathbf{A}\dot{\boldsymbol{\varepsilon}}_t^{\mathrm{th}} \cdot \dot{\boldsymbol{\varepsilon}}_t^{\mathrm{th}} - (1-\beta)^2 \mathbf{A}(\boldsymbol{\varepsilon}(\mathbf{v}) - \boldsymbol{\varepsilon}_t^{\mathrm{th}}) \cdot \ddot{\boldsymbol{\varepsilon}}_t^{\mathrm{th}} \Big)\, \mathrm{d}\mathbf{x}; \tag{18}$$

3. *First directional derivative of $\mathcal{E}_t$ at $(\mathbf{u}, \alpha)$ in the direction $(\mathbf{v}, \beta)$:*

$$\mathcal{E}_t'(\mathbf{u},\alpha)(\mathbf{v},\beta) = \int_\Omega \Big((1-\alpha)^2\mathbf{A}(\boldsymbol{\varepsilon}(\mathbf{u})-\boldsymbol{\varepsilon}_t^{\rm th})\cdot\boldsymbol{\varepsilon}(\mathbf{v}) + \Big(\mathsf{w}-(1-\alpha)\mathbf{A}(\boldsymbol{\varepsilon}(\mathbf{u})-\boldsymbol{\varepsilon}_t^{\rm th})\cdot(\boldsymbol{\varepsilon}(\mathbf{u})-\boldsymbol{\varepsilon}_t^{\rm th})\Big)\beta + \mathsf{w}\ell^2\nabla\alpha\cdot\nabla\beta\Big)\,{\rm d}\mathbf{x}; \tag{19}$$

4. *Second directional derivative of $\mathcal{E}_t$ at $(\mathbf{u},\alpha)$ in the direction $(\mathbf{v},\beta)$:*

$$\mathcal{E}_t''(\mathbf{u},\alpha)(\mathbf{v},\beta) = \int_\Omega \Big((1-\alpha)^2\mathbf{A}\boldsymbol{\varepsilon}(\mathbf{v})\cdot\boldsymbol{\varepsilon}(\mathbf{v}) - 4(1-\alpha)\mathbf{A}(\boldsymbol{\varepsilon}(\mathbf{u})-\boldsymbol{\varepsilon}_t^{\rm th})\cdot\boldsymbol{\varepsilon}(\mathbf{v})\beta + \mathbf{A}(\boldsymbol{\varepsilon}(\mathbf{u})-\boldsymbol{\varepsilon}_t^{\rm th})\cdot(\boldsymbol{\varepsilon}(\mathbf{u})-\boldsymbol{\varepsilon}_t^{\rm th})\beta^2 + \mathsf{w}\ell^2\nabla\beta\cdot\nabla\beta\Big)\,{\rm d}\mathbf{x}; \tag{20}$$

In (20), $\mathcal{E}_t''(\mathbf{u},\alpha)$ is considered as a quadratic form. The associated symmetric bilinear form is still denoted by $\mathcal{E}_t''(\mathbf{u},\alpha)$, but is discriminated by denoting by $\mathcal{E}_t''(\mathbf{u},\alpha)\big\langle(\mathbf{v},\beta),(\bar{\mathbf{v}},\bar\beta)\big\rangle$ its application to a pair of directions. Accordingly, one has $\mathcal{E}_t''(\mathbf{u},\alpha)(\mathbf{v},\beta) = \mathcal{E}_t''(\mathbf{u},\alpha)\,\langle(\mathbf{v},\beta),(\mathbf{v},\beta)\rangle$.

5. *Second order cross term:*

$$\dot{\mathcal{E}}_t'(\mathbf{u},\alpha)(\mathbf{v},\beta) = \int_\Omega \Big(-(1-\alpha)^2\mathbf{A}\dot{\boldsymbol{\varepsilon}}_t^{\rm th}\cdot\boldsymbol{\varepsilon}(\mathbf{v}) + 2(1-\alpha)\mathbf{A}(\boldsymbol{\varepsilon}(\mathbf{u})-\boldsymbol{\varepsilon}_t^{\rm th})\cdot\dot{\boldsymbol{\varepsilon}}_t^{\rm th}\beta\Big)\,{\rm d}\mathbf{x}. \tag{21}$$

2.3. The damage evolution law

Following the variational approach presented in Pham and Marigo (2010a,b), the evolution of the damage in the body is governed by the three principles of irreversibility, stability and energy balance. Specifically, in the present context these conditions read as follows:

Damage law. *The damage evolution is governed by the three following conditions*

(IR) **Irreversibility:** *$t\mapsto\alpha_t$ must be non decreasing and, at each time $t\geq 0$, $\alpha_t\in\mathcal{D}$.*

(ST) **Stability:** *At each time $t\geq 0$, the real state $(\mathbf{u}_t,\alpha_t)\in\mathcal{C}\times\mathcal{D}$ must be stable in the sense that for all $\mathbf{v}\in\mathcal{C}$ and all $\beta\in\mathcal{D}$ such that $\beta\geq\alpha_t$, there exists $\bar h>0$ such that for all $h\in[0,\bar h]$*

$$\mathcal{E}_t(\mathbf{u}_t+h(\mathbf{v}-\mathbf{u}_t),\alpha_t+h(\beta-\alpha_t)) \geq \mathcal{E}_t(\mathbf{u}_t,\alpha_t). \tag{22}$$

(EB) **Energy balance:** *At each time $t\geq 0$ the following energy balance must hold:*

$$\mathcal{E}_t(\mathbf{u}_t,\alpha_t) + \int_0^t\int_\Omega \boldsymbol{\sigma}_s\cdot\dot{\boldsymbol{\varepsilon}}_s^{th}\,{\rm d}\mathbf{x}\,{\rm d}s = 0, \tag{23}$$

where $\boldsymbol{\sigma}_s$ and $\dot{\boldsymbol{\varepsilon}}_s^{th}$ denote respectively the stress field and the rate of the thermal strain field at time s.

An evolution $t\mapsto(\mathbf{u}_t,\alpha_t)$ which starts from $(\mathbf{0},0)$ at time 0 and which satisfies the three conditions above will be called a stable *evolution.*

To simplify the presentation, we will only consider evolutions smooth both in space and time. It is not really a restrictive assumption because we are essentially interested by the loss of uniqueness and of stability of the "fundamental branch" which is smooth as we will see in the next section. Specifically, we make the following smoothness assumption

Hypothesis 1. *We will only consider evolutions such that*

1. *Each component of $\mathbf{u}_t$ and α_t are continuously differentiable in Ω and belong to $H^2(\Omega)$ at every $t\geq 0$;*
2. *$t\mapsto\mathbf{u}_t$ and $t\mapsto\alpha_t$ are continuous and piecewise continuous differentiable. The right and the left time derivatives $\dot{\mathbf{u}}_t^\pm$ and $\dot\alpha_t^\pm$ exist at every time, $\dot{\mathbf{u}}_t^\pm$ belongs to $\mathcal{C}$ and $\dot\alpha_t^\pm$ belongs to $\mathcal{D}^+$, where*

$$\mathcal{D}^+ := H^1(\Omega)\cap\{\beta\geq 0\}.$$

Note that the concept of stability adopted here is that of *directional* stability. For a given admissible direction $(\mathbf{v}, \beta)$, the inequality (22) must hold for sufficiently small h, this neighborhood depending on the direction. Accordingly, for a given direction considering small h and expanding the energy of the perturbed state with respect to h up to the second order, the inequality (22) becomes

$$0 \leq \mathcal{E}_t'(\mathbf{u}_t, \alpha_t)(\mathbf{v} - \mathbf{u}_t, \beta - \alpha_t) + \frac{h}{2}\mathcal{E}_t''(\mathbf{u}_t, \alpha_t)(\mathbf{v} - \mathbf{u}_t, \beta - \alpha_t) + o(h), \tag{24}$$

where $\mathcal{E}_t'$ and $\mathcal{E}_t''$ denote the first and second directional derivatives of $\mathcal{E}_t$. By virtue of Definition 1, one gets

$$\mathcal{E}_t'(\mathbf{u}_t, \alpha_t)(\mathbf{v}, \beta) = \int_\Omega \Big(\boldsymbol{\sigma}_t \cdot \boldsymbol{\varepsilon}(\mathbf{v}) - \mathsf{Y}_t \beta + \mathbf{q}_t \cdot \nabla \beta \Big) \, \mathrm{d}\mathbf{x}, \tag{25}$$

where $\boldsymbol{\sigma}_t$, Y_t and $\mathbf{q}_t$ denote respectively the stress tensor, the energy release rate density and the damage flux vector at time t which are given in terms of the current state by the constitutive relations (6).

Passing to the limit when h goes to 0 in (24) and using the fact that $\mathcal{C}$ is a linear space, one immediately deduces that the stability condition (22) is satisfied *only if*, at each time, the body is at equilibrium and the damage criterion is satisfied. Specifically, these necessary conditions read as

$$\int_\Omega \boldsymbol{\sigma}_t \cdot \boldsymbol{\varepsilon}(\mathbf{v}) \, \mathrm{d}\mathbf{x} = 0, \quad \forall \mathbf{v} \in \mathcal{C}, \tag{26}$$

$$\int_\Omega \left(-\mathsf{Y}_t(\beta - \alpha_t) + \mathbf{q}_t \cdot \nabla(\beta - \alpha_t) \right) \mathrm{d}\mathbf{x} \geq 0, \quad \forall \beta \in \mathcal{D} \ : \ \beta \geq \alpha_t. \tag{27}$$

The two conditions (26)-(27) can be seen as the *first order stability conditions*. They are necessary but not always sufficient in order for (22) to hold. More precisely, if the direction β is such that the inequality is strict in (27), then (24) is satisfied for h small enough and hence the stability is ensured in this direction. However, if the direction β is such that the inequality is an equality in (27), then (24) requires that the second derivative be non negative in order that the state be stable with respect to this direction of perturbation (and the stability in this direction is ensured if the second derivative is positive). We have thus obtained the following

Proposition 1 (Second order stability conditions)**.**

1. *When* $\mathcal{E}_t'(\mathbf{u}_t, \alpha_t)(\mathbf{v} - \mathbf{u}_t, \beta - \alpha_t) > 0$*, then* $(\mathbf{u}_t, \alpha_t)$ *is stable with respect to the direction of perturbation* $(\mathbf{v}, \beta)$*;*
2. *When* $\mathcal{E}_t'(\mathbf{u}_t, \alpha_t)(\mathbf{v} - \mathbf{u}_t, \beta - \alpha_t) = 0$*, then* $(\mathbf{u}_t, \alpha_t)$ *is stable with respect to the direction of perturbation* $(\mathbf{v}, \beta)$*:*
   - if $\mathcal{E}_t''(\mathbf{u}_t, \alpha_t)(\mathbf{v} - \mathbf{u}_t, \beta - \alpha_t) > 0$,
   - only if $\mathcal{E}_t''(\mathbf{u}_t, \alpha_t)(\mathbf{v} - \mathbf{u}_t, \beta - \alpha_t) \geq 0$.

By standard arguments of the calculus of variations and by virtue of Hypothesis 1 of regularity of the fields, one easily deduces from (26)–(27) that the first order stability conditions are satisfied if and only if the following local conditions hold:

$$\operatorname{div} \boldsymbol{\sigma}_t = \mathbf{0} \text{ in } \Omega, \qquad \boldsymbol{\sigma}_t \mathbf{e}_2 = \mathbf{0} \text{ on } x_2 = 0, \qquad \boldsymbol{\sigma}_t \mathbf{e}_1 \cdot \mathbf{e}_2 = 0 \text{ on } x_1 = 0 \text{ or } \mathsf{L}, \tag{28}$$

$$(1 - \alpha_t)\mathbf{A}\boldsymbol{\varepsilon}_t^e \cdot \boldsymbol{\varepsilon}_t^e - \mathsf{w} + \mathsf{w}\ell^2 \Delta \alpha_t \leq 0 \text{ in } \Omega, \qquad \frac{\partial \alpha_t}{\partial n} \geq 0 \text{ on } \partial\Omega. \tag{29}$$

Thus (28) corresponds to the volume equilibrium equations and the natural boundary conditions whereas (29) corresponds to the damage yield criterion. Because of the presence of gradient terms in the energy, the criterion in the bulk involves the second derivatives of the damage field and a natural boundary condition appears involving the normal derivative of the damage field.

Let us use the energy balance (23). Owing to the smoothness assumption on the time evolution, taking the derivative of (23) with respect to t leads to

$$\begin{aligned} 0 &= \frac{d}{dt}\int_\Omega W(\boldsymbol{\varepsilon}(\mathbf{u}_t)-\boldsymbol{\varepsilon}_t^{\rm th},\alpha_t,\nabla\alpha_t)\,\mathrm{d}\mathbf{x}+\int_\Omega \boldsymbol{\sigma}_t\cdot\dot{\boldsymbol{\varepsilon}}_t^{\rm th}\,\mathrm{d}\mathbf{x}\\ &= \int_\Omega \left(\boldsymbol{\sigma}_t\cdot\boldsymbol{\varepsilon}(\dot{\mathbf{u}}_t)-\mathsf{Y}_t\dot\alpha_t+\mathbf{q}_t\cdot\nabla\dot\alpha_t\right)\,\mathrm{d}\mathbf{x}\\ &= -\int_\Omega \Big(\operatorname{div}\boldsymbol{\sigma}_t\cdot\dot{\mathbf{u}}_t+(\mathsf{Y}_t+\operatorname{div}\mathbf{q}_t)\dot\alpha_t\Big)\,\mathrm{d}\mathbf{x}+\int_{\partial\Omega}\Big(\boldsymbol{\sigma}_t\mathbf{n}\cdot\dot{\mathbf{u}}_t+\mathbf{q}_t\cdot\mathbf{n}\dot\alpha_t\Big)\,\mathrm{d}s. \end{aligned} \tag{30}$$

Taking into account the equilibrium and the boundary conditions (28), the terms containing $\boldsymbol{\sigma}_t$ vanish in (30). Therefore, one gets

$$0=-\int_\Omega\Big((1-\alpha_t)\mathbf{A}\boldsymbol{\varepsilon}_t^e\cdot\boldsymbol{\varepsilon}_t^e-\mathsf{w}+\mathsf{w}\ell^2\Delta\alpha_t\Big)\dot\alpha_t\,\mathrm{d}\mathbf{x}+\int_{\partial\Omega}\mathsf{w}\ell^2\frac{\partial\alpha_t}{\partial n}\dot\alpha_t\,\mathrm{d}s. \tag{31}$$

By virtue of the irreversibility conditions and the inequalities (29), the equality (31) holds if an only if the following pointwise equalities hold

$$\Big((1-\alpha_t)\mathbf{A}\boldsymbol{\varepsilon}_t^e\cdot\boldsymbol{\varepsilon}_t^e-\mathsf{w}+\mathsf{w}\ell^2\Delta\alpha_t\Big)\dot\alpha_t=0\text{ in }\Omega,\qquad \frac{\partial\alpha_t}{\partial n}\dot\alpha_t=0\text{ on }\partial\Omega. \tag{32}$$

These equalities can be seen as the local energy balances. They correspond also to what is generally called the consistency relations in Kuhn-Tucker conditions.

We have thus established the

Proposition 2. *A smooth stable evolution $t\mapsto(\mathbf{u}_t,\alpha_t)\in\mathcal{C}\times\mathcal{D}$ must satisfy the following set of local conditions at every time $t\geq 0$ (with the convention that at any time when $t\mapsto\alpha_t$ is not differentiable, the relations hold both for $\dot\alpha_t^-$ and $\dot\alpha_t^+$):*

1. **The Kuhn-Tucker conditions in the bulk**

$$In\ \Omega:\qquad\begin{cases}\dot\alpha_t\geq 0,\\ (1-\alpha_t)\mathbf{A}(\boldsymbol{\varepsilon}(\mathbf{u}_t)-\boldsymbol{\varepsilon}_t^{\rm th})\cdot(\boldsymbol{\varepsilon}(\mathbf{u}_t)-\boldsymbol{\varepsilon}_t^{\rm th})-\mathsf{w}+\mathsf{w}\ell^2\Delta\alpha_t\leq 0,\\ \Big((1-\alpha_t)\mathbf{A}(\boldsymbol{\varepsilon}(\mathbf{u}_t)-\boldsymbol{\varepsilon}_t^{\rm th})\cdot(\boldsymbol{\varepsilon}(\mathbf{u}_t)-\boldsymbol{\varepsilon}_t^{\rm th})-\mathsf{w}+\mathsf{w}\ell^2\Delta\alpha_t\Big)\dot\alpha_t=0.\end{cases}$$

2. **The Kuhn-Tucker conditions on the boundary**

$$On\ \partial\Omega:\qquad \dot\alpha_t\geq 0,\quad \frac{\partial\alpha_t}{\partial n}\geq 0,\quad \frac{\partial\alpha_t}{\partial n}\dot\alpha_t=0.$$

3. **The equilibrium equations and the static boundary conditions**

$$\operatorname{div}\boldsymbol{\sigma}_t=\mathbf{0}\ in\ \Omega,\qquad \boldsymbol{\sigma}_t\mathbf{e}_2=\mathbf{0}\ on\ x_2=0,\qquad \boldsymbol{\sigma}_t\mathbf{e}_1\cdot\mathbf{e}_2=0\ on\ x_1=0\ or\ \mathsf{L}.$$

4. **The stress-strain relation**

$$\boldsymbol{\sigma}_t=(1-\alpha_t)^2\mathbf{A}(\boldsymbol{\varepsilon}(\mathbf{u}_t)-\boldsymbol{\varepsilon}_t^{\rm th})\ in\ \Omega.$$

These conditions are sufficient in order for the irreversibility condition and the energy balance to be satisfied, but not sufficient to verify the full stability condition (22). *Accordingly, a smooth evolution which satisfies only the four conditions above will be called a* stationary *evolution.*

3. The fundamental branch

3.1. The elastic response

Let us consider the elastic response of the plate, *i.e.* the response such that $\alpha_t = 0$ at every t. The stress and strain fields are then given by

$$\boldsymbol{\sigma}_t(\mathbf{x}) = \mathsf{E}\mathsf{a}\vartheta\, \mathsf{f}_\mathsf{c}\Big(\frac{x_2}{2\sqrt{\mathsf{k}_\mathsf{c} t}}\Big)\mathbf{e}_1 \otimes \mathbf{e}_1, \qquad \boldsymbol{\varepsilon}(\mathbf{u}_t)(\mathbf{x}) = -(1+\nu)a\vartheta\, \mathsf{f}_\mathsf{c}\Big(\frac{x_2}{2\sqrt{\mathsf{k}_\mathsf{c} t}}\Big)\mathbf{e}_2 \otimes \mathbf{e}_2, \tag{33}$$

from which one easily deduces $\mathbf{u}_t$ (in particular $\mathbf{u}_t \cdot \mathbf{e}_1 = 0$ and $\mathbf{u}_t \cdot \mathbf{e}_2$ only depends on x_2). Since $|\sigma_{t11}|$ is maximal on the side $x_2 = 0$ where it takes the value $\mathsf{E}\mathsf{a}\vartheta$ at every $t \geq 0$, the damage criterion (29) is satisfied everywhere in Ω at every time if and only if $\mathsf{a}\vartheta \leq \sigma_c/\mathsf{E}$ with $\sigma_\mathsf{c} = \sqrt{\mathsf{w}\mathsf{E}}$ given by (10). Specifically, one has

1. If $\mathsf{E}\mathsf{a}^2\vartheta^2 \leq \mathsf{w}$, then inserting (33) into (19) leads to

$$\mathcal{E}_t'(\mathbf{u}_t, 0)(\mathbf{v} - \mathbf{u}_t, \beta) = \int_\Omega \left(\mathsf{w} - \mathsf{E}\mathsf{a}^2\vartheta^2\, \mathsf{f}_\mathsf{c}\Big(\frac{x_2}{2\sqrt{\mathsf{k}_\mathsf{c} t}}\Big)^2\right)\beta\, \mathrm{d}\mathbf{x}, \qquad \forall t > 0, \forall (\mathbf{v}, \beta) \in \mathcal{C} \times \mathcal{D}.$$

   Since $\mathsf{f}_\mathsf{c}(x)$ decreases from 1 to 0 when x grows from 0 to ∞, $\mathcal{E}_t'(\mathbf{u}_t, \alpha_t)(\mathbf{v} - \mathbf{u}_t, \beta) \geq 0$ and the equality holds if and only if $\beta = 0$ everywhere in Ω. Moreover, by virtue of (20), in such directions the second derivative reads as

$$\mathcal{E}_t''(\mathbf{u}_t, 0)(\mathbf{v} - \mathbf{u}_t, 0) = \int_\Omega \mathbf{A}\boldsymbol{\varepsilon}(\mathbf{v}) \cdot \boldsymbol{\varepsilon}(\mathbf{v})\, \mathrm{d}\mathbf{x}.$$

   Therefore $\mathcal{E}_t''(\mathbf{u}_t, 0)(\mathbf{v} - \mathbf{u}_t, 0) > 0$ for every $\mathbf{v} \in \mathcal{C} \setminus \{0\}$ and hence *the elastic response is stable* at every time $t \geq 0$ in all directions by virtue of Proposition 1.
2. If $\mathsf{E}\mathsf{a}^2\vartheta^2 > \mathsf{w}$, then at every time $t > 0$ there exists a subdomain of Ω where the damage criterion (29) is not satisfied. Hence, *the elastic response is never stable.* Damage occurs as soon as $t > 0$.

3.2. The fundamental branch

From now on we will only consider the case when $\mathsf{a}\vartheta\mathsf{E} > \sigma_\mathsf{c}$ and we introduce the dimensionless loading parameter θ which characterizes the mildness of the thermal shock,

$$\theta = \frac{\sigma_\mathsf{c}}{\mathsf{a}\vartheta\mathsf{E}} < 1. \tag{34}$$

If we consider the elastic response, one sees that the damage criterion is violated in the strip $0 < x_2 < 2\mathsf{f}_\mathsf{c}{}^{-1}(\theta)\sqrt{\mathsf{k}_\mathsf{c} t}$ which grows progressively with time. One can suspect that damage occurs in this strip. Moreover, since the loading and the geometry are invariant with respect to the x_1 direction, one can seek first for an evolution which only depends on x_2 and t. Accordingly, we consider a stationary evolution $(\mathbf{u}_t^*, \alpha_t^*)$ such that α_t^* is of the form

$$\alpha_t^*(\mathbf{x}) = \bar{\alpha}_\tau(y), \quad \tau = \frac{2\sqrt{\mathsf{k}_\mathsf{c} t}}{\theta\ell}, \quad y = \frac{x_2}{2\sqrt{\mathsf{k}_\mathsf{c} t}}, \tag{35}$$

where we have introduced new spatial and time variables inspired by the thermal diffusion process. Inserting this form into (28), it is easy to see that the displacement field is the same as the elastic one and hence

$$\boldsymbol{\varepsilon}(\mathbf{u}_t^*)(\mathbf{x}) = \bar{\boldsymbol{\varepsilon}}_\tau(y) := -(1+\nu)a\vartheta\, \mathsf{f}_\mathsf{c}(y)\mathbf{e}_2 \otimes \mathbf{e}_2. \tag{36}$$

The stress field is different because of the damage evolution

$$\boldsymbol{\sigma}_t^*(\mathbf{x}) = \bar{\boldsymbol{\sigma}}_\tau(y) := (1 - \bar{\alpha}_\tau(y))^2 \mathsf{E}\mathsf{a}\vartheta\, \mathsf{f}_\mathsf{c}(y)\mathbf{e}_1 \otimes \mathbf{e}_1. \tag{37}$$

It remains to find $\bar{\alpha}_\tau$. Assuming that the support of $\bar{\alpha}_\tau$ is the interval $[0, \delta_\tau)$ where δ_τ has to be determined, by virtue of (29) and (32), $\bar{\alpha}_\tau$ must satisfy the following differential equation in this interval

$$\frac{1}{\tau^2}\frac{d^2\bar{\alpha}_\tau}{dy^2}(y) + \mathsf{f}_\mathsf{c}(y)^2(1 - \bar{\alpha}_\tau(y)) = \theta^2 \qquad \forall y \in (0, \delta_\tau). \tag{38}$$

The Kuhn-Tucker condition at $x_2 = 0$ requires that the first derivative of $\bar{\alpha}_\tau$ vanishes at $y = 0$. The continuity of $\bar{\alpha}_\tau$ and of its first derivative at $y = \delta_\tau$ require that both quantities vanish. Therefore the boundary conditions read

$$\frac{d\bar{\alpha}_\tau}{dy}(0) = 0, \qquad \bar{\alpha}_\tau(\delta_\tau) = 0, \qquad \frac{d\bar{\alpha}_\tau}{dy}(\delta_\tau) = 0. \tag{39}$$

Moreover, the damage criterion is satisfied for $y \geq \delta_\tau$ if and only if $\mathsf{f_c}(\delta_\tau) \leq \theta$ and hence if and only if

$$\delta_\tau \geq \mathsf{f_c}^{-1}(\theta). \tag{40}$$

The existence and the uniqueness of $\bar{\alpha}_\tau$ and δ_τ as a solution of (38)–(40) is a consequence of the following

Proposition 3. *At each time $\tau > 0$ the damage field $\bar{\alpha}_\tau$ is necessarily the unique minimizer of $\bar{\mathcal{E}}_\tau$ over $\{\beta \in H^1(0,\infty) : 0 \leq \beta \leq 1\}$, where*

$$\bar{\mathcal{E}}_\tau(\beta) := \int_0^\infty \left(\frac{1}{2\tau^2}\beta'(y)^2 + \frac{1}{2}\mathsf{f_c}(y)^2(1-\beta(y))^2 + \theta^2\beta(y) \right) \mathrm{d}y. \tag{41}$$

Accordingly, the support of $\bar{\alpha}_\tau$ is really a finite interval $[0,\delta_\tau)$ and $(\bar{\alpha}_\tau, \delta_\tau)$ satisfy (38)–(40). Moreover $\bar{\alpha}_\tau$ is monotonically decreasing in $[0,\delta_\tau)$ from $\bar{\alpha}_\tau(0) < 1$ to 0.

Proof. The proof is given in Appendix A. □

From the characterization of $\bar{\alpha}_\tau$, it is easy to obtain its asymptotic behavior at small times and at large times. This leads to the

Proposition 4 (Asymptotic behaviors of $\bar{\alpha}_\tau$)**.**

1. *When τ tends to 0, $(\bar{\alpha}_\tau/\tau^2, \delta_\tau)$ strongly converges in $H^1(0,\infty)\times\mathbb{R}$ to $(\bar{\alpha}_0, \delta_0)$ given by*

$$\delta_0 \text{ is the unique positive number such that } \theta^2\delta_0 = \textstyle\int_0^{\delta_0} \mathsf{f_c}(y)^2\,\mathrm{d}y, \tag{42}$$

$$\begin{cases} \bar{\alpha}_0''(y) = \theta^2 - \mathsf{f_c}(y)^2 & \text{if} \quad y \in [0,\delta_0) \\ \bar{\alpha}_0(y) = 0 & \text{if} \quad y > \delta_0 \end{cases}, \qquad \bar{\alpha}_0(\delta_0) = \bar{\alpha}_0'(\delta_0) = 0. \tag{43}$$

2. *When τ tends to ∞, $(\bar{\alpha}_\tau, \delta_\tau)$ strongly converges in $L^2(0,\infty)\times\mathbb{R}$ to $(\bar{\alpha}_\infty, \delta_\infty)$ given by*

$$\delta_\infty = \mathsf{f_c}^{-1}(\theta), \qquad \bar{\alpha}_\infty(y) = \begin{cases} 1 - \dfrac{\theta^2}{\mathsf{f_c}(y)^2} & \text{if} \quad y \in [0,\delta_\infty) \\ 0 & \text{if} \quad y \geq \delta_\infty \end{cases}. \tag{44}$$

Proof. This result is quite natural in view of (38)-(39). It can be rigorously proved by virtue of Proposition 3 and using classical arguments of functional analysis based on first estimates, weak and strong convergences. The proof is left to the reader. □

In order that $t \mapsto (\mathbf{u}_t^*, \alpha_t^*)$ be an admissible evolution (at least a stationary evolution), it remains to verify that $t \mapsto \alpha_t^*$ satisfies the irreversibility condition, *i.e.* is monotonically increasing. Unfortunately, this property cannot be proved analytically and will be only checked numerically. Indeed, using the chain rule, $\dot{\alpha}_t^*(\mathbf{x})$ reads as

$$\dot{\alpha}_t^*(\mathbf{x}) = \frac{d\bar{\alpha}_\tau}{dy}(y)\frac{\partial y}{\partial t} + \dot{\bar{\alpha}}_\tau(y)\frac{d\tau}{dt}.$$

The first term in the right hand side above is positive because $y \mapsto \bar{\alpha}_\tau(y)$ is monotonically decreasing at given time and y is a decreasing function of t at given x_2. On the other hand, $\tau \mapsto \bar{\alpha}_\tau$ is not monotonically increasing. Indeed, $\tau \mapsto \delta_\tau$ is in fact *monotonically decreasing*. (In particular one immediately deduces from (42) and (44) that $\delta_0 > \delta_\infty$.) Consequently, the second term in the right hand side above is not always positive and one cannot conclude. (In fact we could prove the monotonicity of $t \mapsto \alpha_t^*$ for values of θ close to 1, but not on the full range $(0,1)$.) Accordingly, one adopts the following

Hypothesis 2 (Monotonicity of $t \mapsto \alpha_t^*$)**.** *Throughout the next section we will assume that $t \mapsto \alpha_t^*$ is monotonically increasing and hence that the depth $\mathsf{D}_t^* := 2\delta_\tau\sqrt{\mathsf{k_c}t}$ of the damage zone associated with the fundamental branch is an increasing function of time. Those properties will be checked numerically in Section 5.*

4. Bifurcation from and instability of the fundamental branch

In the wake of Nguyen (1994, 2000) we use bifurcation and stability theory, introduced in the case of non local damage for the selection of solutions in Benallal and Marigo (2007). The response can follow the fundamental branch only as long as the associated state is stable. But the evolution can bifurcate on another branch before the loss of stability of the fundamental branch, whenever such a branch exists and is itself stable (at least in a neighborhood of the bifurcation point). Accordingly, it is important to identify the possible points of bifurcation on the fundamental branch. It is the aim of this section.

4.1. Setting of the rate problem

Let $t > 0$ be a given time and $(\mathbf{u}_t^*, \alpha_t^*)$ be the associated state of the fundamental branch, given by (35)–(40). Let us study the evolution problem in the time interval $[t, t+\eta)$, with $\eta > 0$ and small enough, assuming that the state of the body is the fundamental one $(\mathbf{u}_t^*, \alpha_t^*)$ at time t. Let $\{(\mathbf{u}_s, \alpha_s)\}_{s\in[t,t+\eta)}$ be a possible solution of the evolution problem during the time interval $[t, t+\eta)$. One assumes that the evolution is sufficiently smooth so that the right derivative exists at t. This derivative is denoted $(\dot{\mathbf{u}}, \dot{\alpha})$ and is defined by

$$\dot{\mathbf{u}} = \lim_{h\downarrow 0} \frac{1}{h}(\mathbf{u}_{t+h} - \mathbf{u}_t^*), \qquad \dot{\alpha} = \lim_{h\downarrow 0} \frac{1}{h}(\alpha_{t+h} - \alpha_t^*), \tag{45}$$

these limits being understood in the sense of the natural norm of $\mathcal{C}\times\mathcal{D}$. Moreover, the construction of the rate problem giving $(\dot{\mathbf{u}}, \dot{\alpha})$ needs an additional smoothness assumption relative to the growth of the damage zone. Specifically, one adopts the following

Hypothesis 3 (Smooth growth of the damage zone)**.** *Let Ω_s^d be the damage zone at time $s \in [t, t+\eta)$ in the evolution $\{(\mathbf{u}_s, \alpha_s)\}_{s\in[t,t+\eta)}$, i.e.*

$$\Omega_s^d = \{\mathbf{x} \in \Omega \ : \ \alpha_s(\mathbf{x}) > 0\}. \tag{46}$$

Thus $\Omega_t^d = (0, \mathsf{L})\times[0, \mathsf{D}_t^*)$. By virtue of the irreversibility condition and Hypothesis 2, $s \mapsto \Omega_s^d$ is increasing. One assumes that this growth is smooth in the sense that there exists $C > 0$ such that

$$\Omega_s^d \setminus \Omega_t^d \subset (0, \mathsf{L})\times[\mathsf{D}_t^*, \mathsf{D}_t^* + C(s-t)).$$

Thus, the new damaging points in the time interval (t, s) are included in a strip of width $C(s-t)$.

Of course, if the evolution follows the fundamental branch, then $(\dot{\mathbf{u}}, \dot{\alpha}) = (\dot{\mathbf{u}}_t^*, \dot{\alpha}_t^*)$ and Hypothesis 3 is satisfied because $\tau \mapsto \delta_\tau$ is smooth.

Our purpose is to find whether another rate is possible, recalling that one only considers the case $\theta < 1$. Imposing the evolution to satisfy the three items (IR), (ST) and (EB) and Hypothesis 1, one deduces the following variational formulation for the rate problem.

Proposition 5 (The rate problem)**.** *Let $t > 0$ be a given time. At this time, the rate $(\dot{\mathbf{u}}, \dot{\alpha})$ of any branch which is solution of the evolution problem and follows the fundamental branch up to time t is such that*

$$\begin{aligned} &\dot{\boldsymbol{\chi}} = (\dot{\mathbf{u}}, \dot{\alpha}) \in \mathcal{C}\times\dot{\mathcal{D}}_t^+, \qquad \forall \boldsymbol{\xi} = (\mathbf{v}, \beta) \in \mathcal{C}\times\dot{\mathcal{D}}_t^+ \\ &\quad \mathcal{E}_t''(\boldsymbol{\chi}_t^*)\langle\dot{\boldsymbol{\chi}}, \boldsymbol{\xi} - \dot{\boldsymbol{\chi}}\rangle + \dot{\mathcal{E}}_t'(\boldsymbol{\chi}_t^*)(\boldsymbol{\xi} - \dot{\boldsymbol{\chi}}) \geq 0. \end{aligned} \tag{47}$$

In (47) $\dot{\mathcal{D}}_t^+$ is the set of admissible damage rate fields at time t, i.e.

$$\dot{\mathcal{D}}_t^+ = \{\beta \in H^1(\Omega) : \beta \geq 0 \text{ in } \Omega_t^d, \ \beta = 0 \text{ in } \Omega \setminus \Omega_t^d\}, \qquad \Omega_t^d = (0, \mathsf{L})\times[0, \mathsf{D}_t^*).$$

Proof. The proof is given in Appendix C. □

4.2. Characterization of bifurcation and stability by Rayleigh's ratio minimization

The rate $\dot{\boldsymbol{\chi}}_t^* = (\dot{\mathbf{u}}_t^*, \dot{\alpha}_t^*)$ is solution of (47). The question is to know whether another solution exists. The uniqueness is guaranteed when the quadratic form $\mathcal{E}_t''(\boldsymbol{\chi}_t^*)$ is positive definite on the linear space $\mathcal{C}\times\dot{\mathcal{D}}_t$, $\dot{\mathcal{D}}_t$ denoting the linear space generated by $\dot{\mathcal{D}}_t^+$, *i.e.*

$$\dot{\mathcal{D}}_t = \{\beta \in H^1(\Omega) : \beta = 0 \text{ in } \Omega \setminus \Omega_t^d\}. \tag{48}$$

Indeed, in such a case, let us consider another solution $\dot{\boldsymbol{\chi}}$. Making $\boldsymbol{\xi} = \dot{\boldsymbol{\chi}}_t^*$ in (47) we obtain

$$\mathcal{E}_t''(\boldsymbol{\chi}_t^*)\langle\dot{\boldsymbol{\chi}}, \dot{\boldsymbol{\chi}}_t^* - \dot{\boldsymbol{\chi}}\rangle + \dot{\mathcal{E}}_t'(\boldsymbol{\chi}_t^*)(\dot{\boldsymbol{\chi}}_t^* - \dot{\boldsymbol{\chi}}) \geq 0. \tag{49}$$

Making $\boldsymbol{\xi} = \dot{\boldsymbol{\chi}}$ in the variational inequality satisfied by $\dot{\boldsymbol{\chi}}_t^*$, we get

$$\mathcal{E}_t''(\boldsymbol{\chi}_t^*)\langle\dot{\boldsymbol{\chi}}_t^*, \dot{\boldsymbol{\chi}} - \dot{\boldsymbol{\chi}}_t^*\rangle + \dot{\mathcal{E}}_t'(\boldsymbol{\chi}_t^*)(\dot{\boldsymbol{\chi}} - \dot{\boldsymbol{\chi}}_t^*) \geq 0. \tag{50}$$

The addition of the two inequalities (49)-(50) leads to $\mathcal{E}_t''(\boldsymbol{\chi}_t^*)(\dot{\boldsymbol{\chi}} - \dot{\boldsymbol{\chi}}_t^*) \leq 0$ which is possible only if $\dot{\boldsymbol{\chi}} = \dot{\boldsymbol{\chi}}_t^*$ when $\mathcal{E}_t''(\boldsymbol{\chi}_t^*)$ is positive definite.

Let us now consider the question of the stability of $(\dot{\mathbf{u}}_t^*, \dot{\alpha}_t^*)$. By virtue of Proposition 1, this fundamental state is stable *only if* $\mathcal{E}_t''(\boldsymbol{\chi}_t^*)(\dot{\boldsymbol{\xi}}) \geq 0$, for all $\boldsymbol{\xi} \in \mathcal{C}\times\dot{\mathcal{D}}_t^+$, and *if* $\mathcal{E}_t''(\boldsymbol{\chi}_t^*)(\dot{\boldsymbol{\xi}}) > 0$ for all rates $\dot{\boldsymbol{\xi}} \neq \mathbf{0}$ in $\mathcal{C}\times\dot{\mathcal{D}}_t^+$. Accordingly, the stability is governed by the positivity of $\mathcal{E}_t''(\boldsymbol{\chi}_t^*)$ on $\mathcal{C}\times\dot{\mathcal{D}}_t^+$.

By virtue of (20), $\mathcal{E}_t''(\boldsymbol{\chi}_t^*)$ can be read as the difference of two definite positive quadratic forms on $\mathcal{C}\times\dot{\mathcal{D}}_t$, *i.e.*

$$\mathcal{E}_t''(\boldsymbol{\chi}_t^*) = \mathcal{A}_t^* - \mathcal{B}_t^*$$

with

$$\mathcal{A}_t^*(\mathbf{v}, \beta) = \int_\Omega \Big(\mathbf{A}\big((1-\alpha_t^*)\boldsymbol{\varepsilon}(\mathbf{v}) - 2\boldsymbol{\varepsilon}_t^{e*}\beta\big) \cdot \big((1-\alpha_t^*)\boldsymbol{\varepsilon}(\mathbf{v}) - 2\boldsymbol{\varepsilon}_t^{e*}\beta\big) + \mathsf{w}\ell^2\nabla\beta\cdot\nabla\beta\Big)\,\mathrm{d}\mathbf{x}, \tag{51}$$

$$\mathcal{B}_t^*(\beta) = \int_\Omega 3\mathbf{A}\boldsymbol{\varepsilon}_t^{e*}\cdot\boldsymbol{\varepsilon}_t^{e*}\ \beta^2\,\mathrm{d}\mathbf{x}, \qquad \boldsymbol{\varepsilon}_t^{e*}(\mathbf{x}) = \mathsf{a}\vartheta\,\mathsf{f_c}\Big(\frac{x_2}{2\sqrt{\mathsf{k_c}t}}\Big)(\mathbf{e}_1\otimes\mathbf{e}_1 - \nu\mathbf{e}_2\otimes\mathbf{e}_2). \tag{52}$$

where $\boldsymbol{\varepsilon}_t^{e*}(\mathbf{x})$ comes from (14) and (33). Accordingly, we have:

Proposition 6. *The study of the positivity of $\mathcal{E}_t''$ is equivalent to compare the following Rayleigh ratio $\mathcal{R}_t^*$ with 1:*

$$\mathcal{R}_t^*(\mathbf{v}, \beta) = \begin{cases} \dfrac{\mathcal{A}_t^*(\mathbf{v},\beta)}{\mathcal{B}_t^*(\beta)} & \text{if } \beta \neq 0 \\ +\infty & \text{otherwise} \end{cases}. \tag{53}$$

Specifically, the possibility of bifurcation from the fundamental state is given by

$$\mathsf{R}_t^b := \min_{\mathcal{C}\times\dot{\mathcal{D}}_t} \mathcal{R}_t^*, \qquad \begin{cases} \mathsf{R}_t^b > 1 & \Longrightarrow \quad \textit{no bifurcation} \\ \mathsf{R}_t^b \leq 1 & \Longrightarrow \quad \textit{bifurcation possible} \end{cases} \tag{54}$$

while for the stability of the fundamental state one gets

$$\mathsf{R}_t^s := \min_{\mathcal{C}\times\dot{\mathcal{D}}_t^+} \mathcal{R}_t^*, \qquad \begin{cases} \mathsf{R}_t^s > 1 & \Longrightarrow \quad \textit{stability} \\ \mathsf{R}_t^s < 1 & \Longrightarrow \quad \textit{instability} \end{cases} \tag{55}$$

Remark 1. *By standard arguments one can prove that both minimization problems admit a solution. Since the dependence on time of the fundamental state is smooth, so is the dependence on time of the minima R_t^b and R_t^s. Since $\dot{\mathcal{D}}_t^+ \subset \dot{\mathcal{D}}_t$, one immediately gets $\mathsf{R}_t^b \leq \mathsf{R}_t^s$ and hence one can suspect that a bifurcation occurs before the instability. The proof of that result as well as the determination of the times t_b and t_s when the bifurcation and the loss of stability occur are the aim of the next subsections.*

The bifurcated branch is only observed if it corresponds to stable states. Thus the following result characterizes the neighboring states after bifurcation from the stable fundamental branch.

Proposition 7. *Let $(\mathbf{u}_t^*, \alpha_t^*)$ be the state of the fundamental branch at time $t < t_s$. Let $s \mapsto (\mathbf{u}_s, \alpha_s)$ be a stationary evolution (as defined in Proposition 2) in the time interval $[t, t+\eta)$ which starts from $(\mathbf{u}_t^*, \alpha_t^*)$ at time t. Then for η sufficiently small, all the states of this branch satisfy* (ST) *and are thus stable.*

Proof. The proof is given in Appendix B. □

4.3. Some properties of Rayleigh's ratio minimizations

Let $\hat{\boldsymbol{\xi}} = (\hat{\mathbf{v}}, \hat{\beta})$ be a minimizer of $\mathcal{R}_t^*$ over $\mathcal{C}\times\dot{\mathcal{D}}_t$. It satisfies the following optimal conditions which involve the symmetric bilinear forms $\mathcal{A}_t^*\langle\cdot,\cdot\rangle$ and $\mathcal{B}_t^*\langle\cdot,\cdot\rangle$ associated with the quadratic forms $\mathcal{A}_t^*(\cdot)$ and $\mathcal{B}_t^*(\cdot)$:

$$\mathcal{A}_t^*\langle\hat{\boldsymbol{\xi}}, \boldsymbol{\xi}\rangle = \mathsf{R}_t^b \; \mathcal{B}_t^*\langle\hat{\beta}, \beta\rangle, \qquad \forall \boldsymbol{\xi} = (\mathbf{v}, \beta) \in \mathcal{C}\times\dot{\mathcal{D}}_t. \tag{56}$$

By standard arguments, one deduces the natural boundary conditions $\partial\hat{\beta}/\partial x_1 = 0$ on $x_1 = 0$ or L. Therefore, as it is suggested by the x_1 independence of the fundamental state, one can decompose $\hat{\beta}$ into the following Fourier series:

$$\hat{\beta}(\mathbf{x}) = \sum_{k\in\mathbb{N}} \hat{\beta}^k(\zeta)\cos\left(k\pi\frac{x_1}{\mathsf{L}}\right), \qquad \zeta = \frac{x_2}{\mathsf{D}_t^*}, \tag{57}$$

where one introduces the change of coordinate $x_2 \mapsto \zeta$ in order that the support of the functions $\hat{\beta}^k$ be the fix interval $[0, 1)$. Accordingly, the $\hat{\beta}^k$'s can be seen as elements of $\mathcal{H}_0$,

$$\mathcal{H}_0 = \{\beta \in H^1(0,1) : \beta(1) = 0\}.$$

In the same way, using the boundary conditions $\hat{v}_1 = 0$, $\varepsilon_{12}(\hat{\mathbf{v}}) = 0$ and hence $\partial\hat{v}_2/\partial x_1 = 0$ on $x_1 = 0$ or L, $\hat{\mathbf{v}}$ can be decomposed as follows:

$$\hat{\mathbf{v}}(\mathbf{x}) = \sum_{k\in\mathbb{N}} 2\mathsf{a}\vartheta\delta_\tau\sqrt{\mathsf{k_c}t}\left(\hat{V}_1^k(\zeta)\sin\left(k\pi\frac{x_1}{\mathsf{L}}\right)\mathbf{e}_1 + \hat{V}_2^k(\zeta)\cos\left(k\pi\frac{x_1}{\mathsf{L}}\right)\mathbf{e}_2\right) \tag{58}$$

where the $\hat{\mathbf{V}}^k$'s are normalized to simplify future expressions and belong to $\mathbf{H}$,

$$\mathbf{H} = H^1(0,\infty)^2.$$

Considering only the rates $(\mathbf{v}, \beta)$ in $\mathcal{C}\times\dot{\mathcal{D}}_t$ which can be decomposed in the same manner and using the orthogonality between the trigonometric functions of x_1 entering in the expansions of $(\mathbf{v}, \beta)$, the different modes $(\mathbf{V}^k, \beta^k)$ are uncoupled from each other. Specifically $\mathcal{A}_t^*$ and $\mathcal{B}_t^*$ can read as

$$\mathcal{A}_t^*(\mathbf{v}, \beta) = \sum_{k\in\mathbb{N}} \mathcal{A}_t^k(\mathbf{V}^k, \beta^k) \qquad \mathcal{B}_t^*(\beta) = \sum_{k\in\mathbb{N}} \mathcal{B}_t^k(\beta^k).$$

Therefore, if one introduces the Rayleigh ratios $\mathcal{R}_t^k(\mathbf{V}, \beta) = \mathcal{A}_t^k(\mathbf{V}, \beta)/\mathcal{B}_t^k(\beta)$ for $k \in \mathbb{N}$, then

$$\mathsf{R}_t^b = \min_{k\in\mathbb{N}} \min_{\mathbf{H}\times\mathcal{H}_0} \mathcal{R}_t^k. \tag{59}$$

Indeed, let $\hat{\mathsf{R}}_t^k$ be the minimum of $\mathcal{R}_t^k$ over $\mathbf{H}\times\mathcal{H}_0$ and let $(\hat{V}_t^k, \hat{\beta}_t^k)$ be a minimizer. Let $\hat{k}_t$ be a minimizer of $k \mapsto \hat{\mathsf{R}}_t^k$. (All these minimizers exist.) Then $\mathcal{A}_t^k(\mathbf{V}, \beta) \geq \hat{\mathsf{R}}_t^{\hat{k}_t}\mathcal{B}_t^k(\beta)$ for all $k \in \mathbb{N}$ and all $(\mathbf{V}, \beta) \in \mathbf{H}\times\mathcal{H}_0$. Therefore, $\mathsf{R}_t^b \geq \hat{\mathsf{R}}_t^{\hat{k}_t}$. But since $\hat{\mathsf{R}}_t^{\hat{k}_t} = \mathcal{R}_t^*(\hat{V}_t^{\hat{k}_t}, \hat{\beta}_t^{\hat{k}_t})$, one gets $\hat{\mathsf{R}}_t^{\hat{k}_t} \geq \mathsf{R}_t^b$ and hence $\hat{\mathsf{R}}_t^{\hat{k}_t} = \mathsf{R}_t^b$.

Finally, after a last change of variable (63) and introducing the assumption that the internal length ℓ is small by comparison with the width of the body L, we are in a position to set the following

Proposition 8. *Assuming that $\ell \ll \mathsf{L}$, at a given time $t > 0$, the minimum of the Rayleigh ratio $\mathcal{R}_t^*$ over $\mathcal{C}\times\dot{\mathcal{D}}_t$ is given by*

$$\mathsf{R}_t^b = \min_{\kappa\geq 0}\min_{\mathbf{H}\times\mathcal{H}_0} \bar{\mathcal{R}}_\tau^\kappa, \qquad \bar{\mathcal{R}}_\tau^\kappa(\mathbf{V},\beta) = \begin{cases} \dfrac{\bar{\mathcal{A}}_\tau^\kappa(\mathbf{V},\beta)}{\bar{\mathcal{B}}_\tau(\beta)} & \text{if } \beta \neq 0 \\ +\infty & \text{otherwise} \end{cases}, \tag{60}$$

where the dimensionless quadratic forms $\bar{\mathcal{A}}_\tau^\kappa$ and $\bar{\mathcal{B}}_\tau$ are given by

$$\begin{aligned} \bar{\mathcal{A}}_\tau^\kappa(\mathbf{V},\beta) &= \int_0^\infty \frac{(1-\bar{\alpha}_\tau(\delta_\tau\zeta))^2}{1-\nu^2}\left(\kappa^2 V_1(\zeta)^2 + V_2'(\zeta)^2 + 2\nu\kappa V_1(\zeta)V_2'(\zeta) + \frac{1-\nu}{2}\Big(V_1'(\zeta)+\kappa V_2(\zeta)\Big)^2\right)\mathrm{d}\zeta \\ &\quad + \int_0^1 \Big(-4(1-\bar{\alpha}_\tau(\delta_\tau\zeta))\mathsf{f}_\mathsf{c}(\delta_\tau\zeta)\kappa V_1(\zeta)\beta(\zeta) + 4\mathsf{f}_\mathsf{c}(\delta_\tau\zeta)^2\beta(\zeta)^2\Big)\mathrm{d}\zeta \\ &\quad + \frac{1}{\delta_\tau^2\tau^2}\int_0^1 \Big(\kappa^2\beta(\zeta)^2 + \beta'(\zeta)^2\Big)\mathrm{d}\zeta, \end{aligned} \tag{61}$$

$$\bar{\mathcal{B}}_\tau(\beta) = \int_0^1 3\mathsf{f}_\mathsf{c}(\delta_\tau\zeta)^2\beta(\zeta)^2\,\mathrm{d}\zeta. \tag{62}$$

The optimal "wave number" $\hat{k}_t$ is related to the optimal dimensionless "wave number" $\hat{\kappa}_\tau$ (minimizer of $\bar{\mathcal{R}}_\tau^\kappa$) by

$$\hat{k}_t = \frac{\hat{\kappa}_\tau}{\pi\theta\delta_\tau\tau}\frac{\mathsf{L}}{\ell}, \quad \tau = \frac{2\sqrt{\mathsf{k_c}t}}{\theta\ell}, \tag{63}$$

and, since $\ell \ll \mathsf{L}$, the discrete minimization problem over $\mathbb{N}$ for k can be replaced by a continuous minimization problem over $\mathbb{R}^+$ for κ.

Proof. The change of variable $\zeta = x_2/\mathsf{D}_t^*$ reduces the support of β to $[0,1)$. By virtue of (59), it suffices to insert (57) and (58) into (51)–(53) to obtain after some calculations (60)–(63). □

The next Proposition gives some useful estimates of the Rayleigh ratio minima.

Proposition 9 (Some estimates of R_t^b, $\min_{\mathbf{H}\times\mathcal{H}_0}\bar{\mathcal{R}}_\tau^\kappa$ and R_t^s)**.**

1. *There exists $C > 0$ such that $\min_{\mathbf{H}\times\mathcal{H}_0}\bar{\mathcal{R}}_\tau^\kappa \geq \dfrac{C}{\tau^2}$ for all $\tau > 0$ and all $\kappa \geq 0$;*
2. $\lim_{t\to 0}\mathsf{R}_t^b = \lim_{\tau\to 0}\left(\min_{\mathbf{H}\times\mathcal{H}_0}\bar{\mathcal{R}}_\tau^\kappa\right) = +\infty$, $\forall\kappa \geq 0$*;*
3. $\lim_{t\to\infty}\mathsf{R}_t^b \leq \lim_{t\to\infty}\mathsf{R}_t^s < 1$*;*
4. $\min_{\mathbf{H}\times\mathcal{H}_0}\mathcal{R}_\tau^0 \geq 4/3$, $\forall\tau > 0$. *Moreover,* $\lim_{\tau\to\infty}\min_{\mathbf{H}\times\mathcal{H}_0}\mathcal{R}_\tau^0 = 4/3$.
5. *For given $\tau > 0$,*

$$\lim_{\kappa\to\infty}\frac{\min_{\mathbf{H}\times\mathcal{H}_0}\bar{\mathcal{R}}_\tau^\kappa}{\kappa^2} = \frac{1}{3\delta_\tau^2\tau^2}.$$

Proof. The proof is given in Appendix D. □

4.4. Determination of the first bifurcation

We are now in a position to obtain the major result of this paper.

Proposition 10. *There exists a time $t_b > 0$ such that $\mathsf{R}_t^b > 1, \forall t < t_b$ and $\mathsf{R}_{t_b}^b = 1$. Therefore t_b is the first time at which a bifurcation from the fundamental branch can occur. The fundamental branch is still stable at this time but becomes definitively unstable at a time t_s such that $t_b < t_s < +\infty$.*

Moreover, at time t_b, the rate problem admits other solutions than the rate $(\dot{\mathbf{u}}_{t_b}^*, \dot{\alpha}_{t_b}^*)$ corresponding to the fundamental branch. Such bifurcation rates $(\dot{\mathbf{u}}, \dot{\alpha})$ are necessarily of the following form

$$(\dot{\mathbf{u}}, \dot{\alpha}) = (\dot{\mathbf{u}}_{t_b}^*, \dot{\alpha}_{t_b}^*) + c\,(\mathbf{v}^b, \beta^b) \tag{64}$$

where $(\mathbf{v}^b, \beta^b)$ *is a minimizer of* $\mathcal{R}^*_{t_b}$ *over* $\mathcal{C}\times\dot{\mathcal{D}}_{t_b}$ *while* c *is an arbitrary (but non-zero) constant whose absolute value is sufficiently small so that* $\dot\alpha^*_{t_b} + c\,\beta^b \geq 0$. *Conversely, if* $(\mathbf{v}^b, \beta^b)$ *is a minimizer of* $\mathcal{R}^*_{t_b}$ *over* $\mathcal{C}\times\dot{\mathcal{D}}_{t_b}$, *then there exists* $\bar c > 0$ *such that, for every* c *with* $|c| \leq \bar c$, $(\dot{\mathbf{u}}, \dot\alpha)$ *given by* (64) *is really solution of the rate problem at* t_b.

Specifically, the time t_b *and the mode of bifurcation* $(\mathbf{v}^b, \beta^b)$ *are given by*

$$t_b = \frac{\theta^2\tau_b^2\ell^2}{4\mathsf{k_c}}, \tag{65}$$

$$\mathbf{v}^b(\mathbf{x}) = \mathsf{a}\vartheta\mathsf{D}_b\left(\hat V_1^b\Big(\frac{x_2}{\mathsf{D}_b}\Big)\sin\left(2\pi\frac{x_1}{\lambda_b}\right)\mathbf{e}_1 + \hat V_2^b\Big(\frac{x_2}{\mathsf{D}_b}\Big)\cos\left(2\pi\frac{x_1}{\lambda_b}\right)\mathbf{e}_2\right), \tag{66}$$

$$\beta^b(\mathbf{x}) = \hat\beta^b\Big(\frac{x_2}{\mathsf{D}_b}\Big)\cos\left(2\pi\frac{x_1}{\lambda_b}\right). \tag{67}$$

In (65)–(67) *the wave number* κ_b *and the modes* $(\hat{\mathbf{V}}^b, \hat\beta^b)$ *are (normalized) minimizers of* $\bar{\mathcal{R}}^\kappa_{\tau_b}(\mathbf{V}, \beta)$ *over all* $\kappa \geq 0$ *and all* $(\mathbf{V}, \beta) \in \mathbf{H}\times\mathcal{H}_0$ *while* τ_b *is such that* $\bar{\mathcal{R}}^{\kappa_b}_{\tau_b}(\hat{\mathbf{V}}^b, \hat\beta^b) = 1$. *Since* $0 < \kappa_b < +\infty$, *the damage mode of bifurcation is a sinusoid with respect to* x_1 *whose wavelength* λ_b *is finite and given by*

$$\lambda_b = 2\pi\frac{\theta\delta_{\tau_b}\tau_b}{\kappa_b}\ell. \tag{68}$$

In (66)-(67), D_b *represents the depth of the damage zone at time* t_b, *i.e.*

$$\mathsf{D}_b := 2\delta_{\tau_b}\sqrt{\mathsf{k_c}t_b} = \theta\delta_{\tau_b}\tau_b\ell. \tag{69}$$

Hence, λ_b *and* D_b *are proportional to the internal length* ℓ *of the material. The coefficients of proportionality only depend on the Poisson ratio* ν *and on the dimensionless parameter* θ *characterizing the amplitude of the thermal shock.*

Proof. The proof is divided into 3 steps.

(i) : *Definitions of* t_b *and* t_s. By virtue of Proposition 9 (Properties 2 and 3), R^b_t varies continuously from a value less than 1 to $+\infty$ when t goes from 0 to $+\infty$. Hence, there exists at least one time s such that $\mathsf{R}^b_s = 1$. Any such time is necessarily non-zero and finite, *i.e.* $0 < s < +\infty$. Defining t_b as the smallest of such times, one gets $\mathsf{R}^b_t > 1$ for all $t < t_b$ by virtue of Property 2. Therefore, by virtue of (54), t_b is the first time when a bifurcation can occur.

In the same way, since $\mathsf{R}^s_t \geq \mathsf{R}^b_t$ and by virtue of the Properties 2 and 3, R^s_t varies continuously from a value less than 1 to $+\infty$ when t goes from 0 to $+\infty$. Hence there exists at least one time σ such that $\mathsf{R}^s_\sigma = 1$. Any such time is necessarily non-zero and finite, *i.e.* $0 < \sigma < +\infty$. Defining t_s as the largest of such times, one gets $\mathsf{R}^s_t < 1$ for all $t > t_s$ by virtue of Property 3. Therefore, by virtue of (55), the fundamental branch is never stable after t_s. Hence, these critical times are such that $0 < t_b \leq t_s < +\infty$. (The inequality $t_b < t_s$ will be proved in the next step.) $\triangleleft$

(ii) : *Necessary form of a bifurcation rate.* Let us consider the rate problem at time t_b and let $\dot{\boldsymbol\chi}$ be a solution. Inserting into (47) and taking into account that $\dot{\boldsymbol\chi}^*_{t_b}$ itself satisfies (47) at time t_b gives $\mathcal{A}^*_{t_b}(\dot{\boldsymbol\chi} - \dot{\boldsymbol\chi}^*_{t_b}) \leq \mathcal{B}^*_{t_b}(\dot{\boldsymbol\chi} - \dot{\boldsymbol\chi}^*_{t_b})$, see (49)-(50). But since $\mathsf{R}^s_{t_b} := \min_{\mathcal{C}\times\dot{\mathcal{D}}_{t_b}}\mathcal{R}^*_{t_b} = 1$, one has also the converse inequality and hence the equality

$$\mathcal{A}^*_{t_b}(\dot{\boldsymbol\chi} - \dot{\boldsymbol\chi}^*_{t_b}) = \mathcal{B}^*_{t_b}(\dot{\boldsymbol\chi} - \dot{\boldsymbol\chi}^*_{t_b}).$$

Therefore, if $\dot{\boldsymbol\chi} \neq \dot{\boldsymbol\chi}^*_{t_b}$, then $\dot{\boldsymbol\chi} - \dot{\boldsymbol\chi}^*_{t_b}$ must be a minimizer of $\mathcal{R}^*_{t_b}$ over $\mathcal{C}\times\dot{\mathcal{D}}_{t_b}$. Therefore, by virtue of the analysis of the previous subsection and Proposition 8, $\dot{\boldsymbol\chi}$ must take the form given by (64)–(69). Indeed, $(\kappa_b, \hat V^b, \hat\beta^b)$ is a minimizer of $(\kappa, \mathbf{V}, \beta) \mapsto \bar{\mathcal{R}}^\kappa_{\tau_b}(\mathbf{V}, \beta)$ over $\mathbb{R}^+\times\mathbf{H}\times\mathcal{H}_0$ and $1 = \bar{\mathcal{R}}^{\kappa_b}_{\tau_b}(\kappa_b, \hat V^b, \hat\beta^b)$. By virtue of the properties 4 and 5 of Proposition 9, $0 < \kappa_b < +\infty$ and hence the wave length λ_b is non-zero and finite. By using (63) at time t_b, one obtains (65) and (68). Since, at a given τ, $\bar\alpha_\tau$ depends only on θ, so does δ_τ. Therefore $\bar{\mathcal{R}}^\kappa_\tau$ depends only on ν and θ. Accordingly, κ_b and τ_b depend only on ν and θ.

Since $\lambda_b < +\infty$, the dependence of β^b on x_1 is really sinusoidal and hence β^b does not belong to $\dot{\mathcal{D}}^+_{t_b}$. Accordingly $(\mathbf{v}^b, \beta^b)$ cannot be a minimizer of $\mathcal{R}^*_{t_b}$ over $\mathcal{C}\times\dot{\mathcal{D}}^+_{t_b}$. Therefore $\mathsf{R}^s_{t_b} > 1 = \mathsf{R}^b_{t_b}$ and hence $t_s > t_b$. The fundamental branch is still stable at t_b. $\triangleleft$

(iii) : *Existence of a bifurcation rate.* It remains to prove that non trivial solutions for the rate problem really exist at time t_b. So, let $(\kappa_b, \hat{V}^b, \hat{\beta}^b)$ be a minimizer of $(\kappa, \mathbf{V}, \beta) \mapsto \bar{\mathcal{R}}^\kappa_{\tau_b}(\mathbf{V}, \beta)$ over $\mathbb{R}^+\times\mathbf{H}\times\mathcal{H}_0$. Since $(\kappa_b, c\hat{V}^b, c\hat{\beta}^b)$ is also a minimizer for any $c \neq 0$ and since $\hat{\beta}^b \neq 0$, one can normalize the minimizer for instance by $\int_0^1 \hat{\beta}^b(\zeta)^2\,\mathrm{d}\zeta = 1$. Let us consider the rate $\dot{\boldsymbol{\chi}} = \dot{\boldsymbol{\chi}}^*_{t_b} + c\boldsymbol{\xi}^b$ with $\boldsymbol{\xi}^b = (\mathbf{v}^b, \beta^b)$ given by (66)-(67) and $c \neq 0$. Since $\boldsymbol{\xi}^b$ is a minimizer of $\mathcal{R}^*_{t_b}$ over $\mathcal{C}\times\dot{\mathcal{D}}_{t_b}$ and since $\mathsf{R}^b_{t_b} = 1$, $\boldsymbol{\xi}^b$ satisfies the variational equality

$$\mathcal{E}''_{t_b}(\boldsymbol{\chi}^*_{t_b})\langle\boldsymbol{\xi}^b, \boldsymbol{\xi}\rangle = 0, \quad \forall\boldsymbol{\xi} \in \mathcal{C}\times\dot{\mathcal{D}}_{t_b}. \tag{70}$$

Since $\dot{\boldsymbol{\chi}}^*_{t_b}$ is solution of the rate problem, it satisfies (47) which reads at time t_b as

$$\mathcal{E}''_{t_b}(\boldsymbol{\chi}^*_{t_b})\langle\dot{\boldsymbol{\chi}}^*_{t_b}, \boldsymbol{\xi} - \dot{\boldsymbol{\chi}}^*_{t_b}\rangle + \dot{\mathcal{E}}'_{t_b}(\boldsymbol{\chi}^*_{t_b})(\boldsymbol{\xi} - \dot{\boldsymbol{\chi}}^*_{t_b}) \geq 0, \quad \forall\boldsymbol{\xi} \in \mathcal{C}\times\dot{\mathcal{D}}^+_{t_b}. \tag{71}$$

Using (21), (66) and (67), it turns out that $\dot{\mathcal{E}}'_{t_b}(\boldsymbol{\chi}^*_{t_b})(\boldsymbol{\xi}^b) = 0$. Indeed, by virtue of the independence of $\varepsilon^{\mathrm{th}}_t$ and α^*_t on x_1, one gets

$$\dot{\mathcal{E}}'_{t_b}(\boldsymbol{\chi}^*_{t_b})(\boldsymbol{\xi}^b) = \int_0^\infty\int_0^L \phi(\zeta)\cos\left(k_b\pi\frac{x_1}{L}\right)\mathrm{d}x_1\,\mathrm{d}\zeta = 0. \tag{72}$$

Therefore, after calculations based on (70)–(72), one obtains $\forall\boldsymbol{\xi} \in \mathcal{C}\times\dot{\mathcal{D}}^+_{t_b}$:

$$\mathcal{E}''_{t_b}(\boldsymbol{\chi}^*_{t_b})\langle\dot{\boldsymbol{\chi}}, \boldsymbol{\xi} - \dot{\boldsymbol{\chi}}\rangle + \dot{\mathcal{E}}'_{t_b}(\boldsymbol{\chi}^*_{t_b})(\boldsymbol{\xi} - \dot{\boldsymbol{\chi}}) = \mathcal{E}''_{t_b}(\boldsymbol{\chi}^*_{t_b})\langle\dot{\boldsymbol{\chi}}^*_{t_b}, \boldsymbol{\xi} - \dot{\boldsymbol{\chi}}^*_{t_b}\rangle + \dot{\mathcal{E}}'_{t_b}(\boldsymbol{\chi}^*_{t_b})(\boldsymbol{\xi} - \dot{\boldsymbol{\chi}}^*_{t_b}) \geq 0, \tag{73}$$

and hence $\dot{\boldsymbol{\chi}}$ satisfies (47) at t_b. In order that $\dot{\boldsymbol{\chi}}$ be a solution of the rate problem, it remains to verify that $\dot{\alpha}^*_{t_b} + c\beta^b \geq 0$. Since it is true for sufficiently small $|c|$ (one has to prove that $\dot{\alpha}'$ is non zero and that β' is finite. This proof is left to the reader), one has constructed a family of non trivial solutions of the rate problem at time t_b. $\triangleleft$ The proof of the Proposition is complete. $\square$

5. Numerical results

This section is devoted to the numerical exploration of the equations of the minimization problem. These results can be classified in three families: illustration, hypothesis validation and quantification. Some results are illustrated by plotting the solutions. The validation of hypothesis can be made numerically such as the irreversibility. The main interest is to quantify the results especially those of Proposition 10 with the wavelength at the first bifurcation. This numerical implementation is based on two aspects: solving (38) by a shoot method and minimizing (60). Before starting, let us recall that the loading parameter reads $\theta = \sigma_{\mathsf{c}}/(\mathsf{a}\vartheta E)$, and thus $\theta \to 0$ correspond to a extremely severe thermal shock and $\theta \to 1$ to a mild shock.

5.1. The fundamental branch

The fundamental branch is a solution with homogenous damage in the direction parallel to the surface of the thermal shock. It exists for any positive time $t > 0$ and has non-zero damage in a strip within a positive distance D^*_t from the surface. Using the time and space variables τ and y adapted to the thermal problem (Table 1), the value of the damage field in the region $0 < y < \delta_\tau = D^*_t/2\sqrt{\mathsf{k_c}t}$ is found by solving the second order non-autonomous linear differential equation (38) with the boundary conditions (39). The existence and uniqueness of the solution of this boundary value problem is guaranteed by Proposition 4. To solve it, for a given time τ and mildness of thermal shock θ, we apply a shooting method, which, after solving the initial value problem for $\bar{\alpha}_\tau(\delta_\tau) = \bar{\alpha}'_\tau(\delta_\tau) = 0$, searches for the length of the damaged domain δ_τ such that $\bar{\alpha}'_\tau(0) = 0$. The corresponding solution for δ_τ is checked against the asymptotic results for δ_0 and

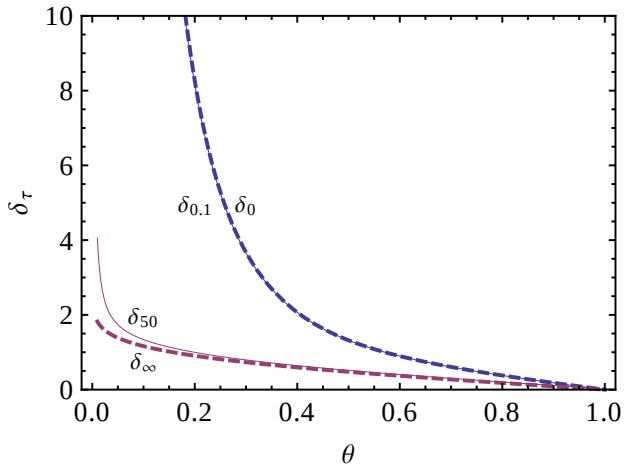

Figure 4: Asymptotic result for the scaled depth of the damage strip δ_τ as a function of the mildness thermal shock θ. The dashed lines are the results for $\tau \to 0$, δ_0, and for $\tau \to \infty$, δ_∞. The continuous lines are the results of the numerical root finding in the shooting method for short ($\tau = 0.1$) and long ($\tau = 50$) times.

δ_∞ obtained in Proposition 4 (Fig. 4). For large values of τ, the numerical problem becomes ill-conditioned and differential solver and root finding algorithms show convergence issues.

Figure 5 reports the damage field obtained for different times and thermal shock intensities. The left and right columns show the results in the scaled (y,τ) and physical ($\mathbf{x}$,t) coordinates, respectively. This fundamental solution is independent of the Poisson ratio ν, being characterized by null displacements in the x_1-direction. At this stage nothing can be said on the uniqueness and stability of these fundamental solutions.

The damage is non null for any positive time. For severe thermal shocks (see the plots at the top for $\theta = 0.01$ in the figure), the solution in the physical space is characterized by an almost fully damaged zone close to the boundary, which propagates inside the domain with increasing time. For mild thermal shock ($\theta = 0.5, 0.9$) the solution is with smaller space and time gradients. Note that δ_τ is decreasing with τ, whilst D_t^* is increasing with t. For any value of θ and τ, the solution is monotonically decreasing in space, varying from a maximum value $\alpha_t^*(0)$ at the boundary to 0 at $x = D_t^*$, as proven in Proposition 3. Hence, its behavior as a function of θ and t can be globally resumed by the contour-plots of the damage at the surface, $\alpha_t^*(0)$, and the length of the damaged domain, D_t^*, see Figure 6. Both the maximal value of the damage field and the damage penetration depth increase monotonically with the severity of the thermal shock and the time. The limit value of the maximal value of the damage field for $t, \tau \to \infty$ is $\alpha_\infty^*(0) = 1 - \theta^2 < 1$ (see Proposition 4, Eqns. (44)). To check numerically that the solution $\alpha_t^*(x_2)$ respects the irreversibility condition for a fixed loading θ, we report in Figure 7 $\dot{\alpha}_t^*(x_2)$ as a function of x_2 and t for $\theta = 0.2$. Similar results are found for any other tested value of θ. In particular, for any value of θ, whenever the numerical ODE solver converges, we get that the minimum value of $\dot{\alpha}_t^*(x_2)$ over $t > 0, x_2 > 0$ is 0. The numerical tests seem to corroborate the validity of Hypothesis 2 on the irreversibility of the fundamental branch.

5.2. Bifurcation from the fundamental branch: critical times, critical damage penetration and optimal wavelength

The goal of this Section is to quantify numerically the first possible bifurcation from the fundamental branch. Starting from the result of Proposition 8, we solve the problem using the partial Fourier series in the x_1-variable and the associated wave number κ introduced in Section 4.3, Eqns. (57)-(58). For the x_2-direction, we use the dimensionless variables $\zeta = x_2/\mathsf{D}_t^*$, so that the support of the damaged strip of the fundamental solution is $[0, 1)$ for any loading parameter θ. Hence, we study numerically the sign of the second derivative of the energy $\mathcal{E}_t''(\boldsymbol{\chi}_t^*)$, which below is referred to as $\mathcal{E}_t''$ for brevity, and look for the critical

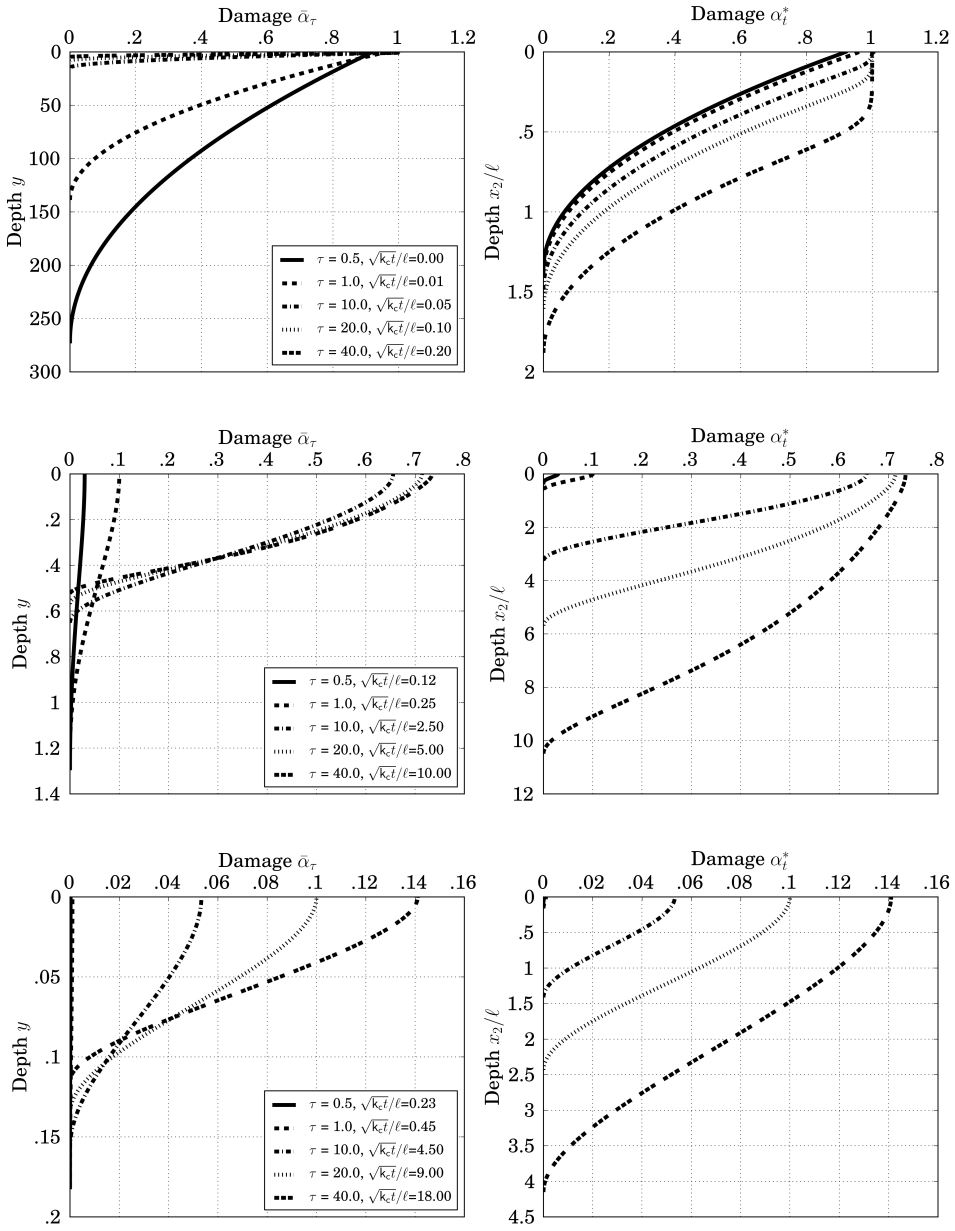

Figure 5: Fundamental solution in the physical space and in the spatial coordinates defined (35). The loading parameter takes the values $\theta = \{.01, .5, .9\}$ (top to bottom). The list of rescaled times $\tau = \{.5, 1, 10, 20, 40\}$ are the same for all 3 loading corresponding to different dimensionless physical time $\sqrt{\mathsf{k_c} t}/\ell$

bifurcation times τ_b, the critical wave numbers κ_b and the associated bifurcation modes as a function of the thermal shock mildness θ.

In the numerical work, the study of the positive definiteness of $\mathcal{E}_t''$ is based on the following Proposition.

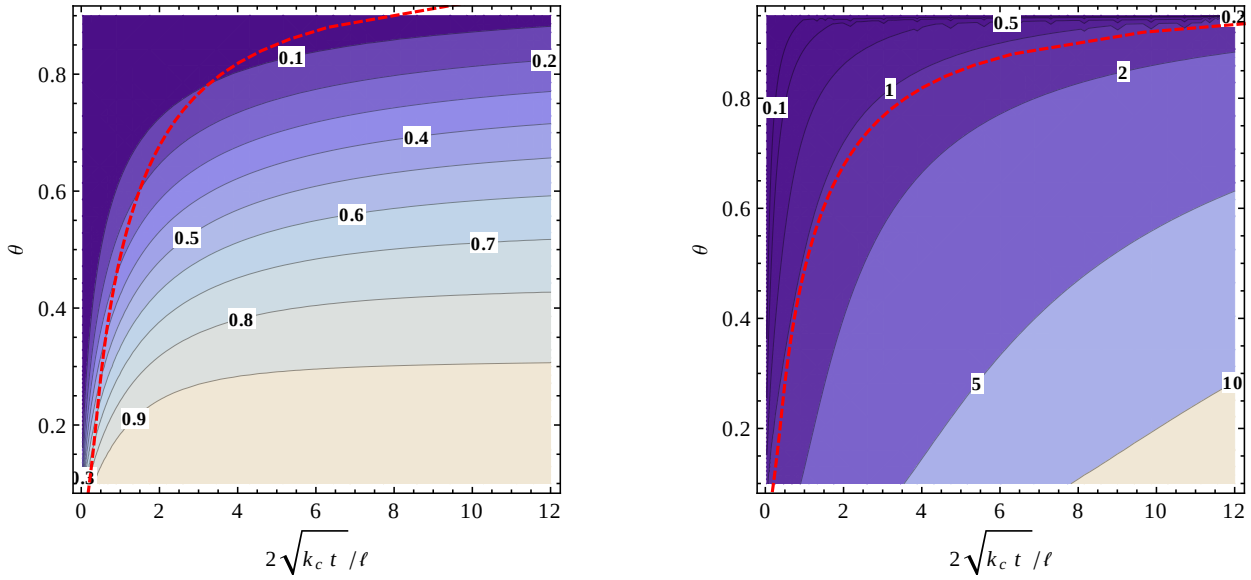

(a) $\alpha_t^*(0)$ (b) D_t^*/ℓ

Figure 6: Fundamental solution: damage at the surface $\alpha_t^*(0)$ and penetration of the damage D_t^* of the fundamental solution as a function of the thermal shock mildness (θ) and time. The red dashed line indicates the bifurcation time as a function of θ and separates the parameter space in regions where the fundamental solution is unique or not.

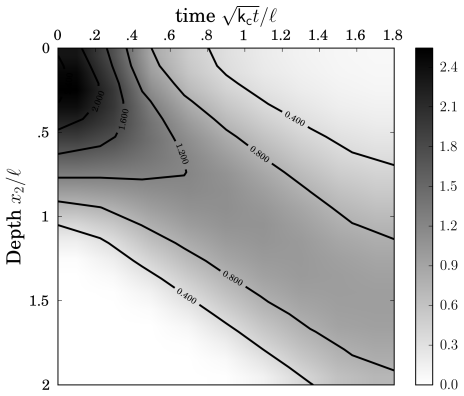

Figure 7: Check of the irreversibility condition: Total time derivative of the damage field of the fundamental branch α_t^* with respect to time, $\dot{\alpha}_t^*$, for the loading $\theta = .2$.

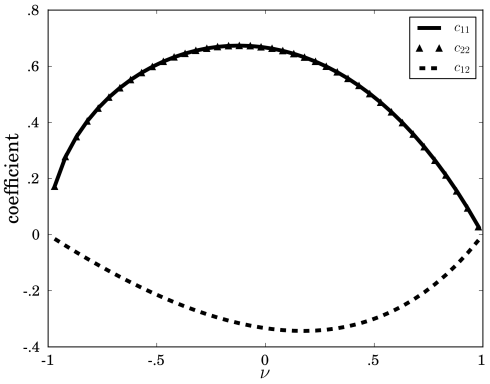

Figure 8: Dependence of the coefficients c_{11}, c_{12}, c_{22} defined by (75) with respect to the Poisson ratio ν.

Proposition 11. *Let*

$$\left\{\mu_i, (\mathbf{V}^{(i)}, \beta^{(i)})\right\}_{i=1}^{\infty}, \qquad \mu_i \leq \mu_{i+1}$$

be the eigenvalues and the eigenvectors of the following quadratic form defined on the finite interval $[0,1]$

$$\tilde{\mathcal{E}}''_\tau(\mathbf{V},\beta) = \tilde{\mathcal{A}}^\kappa_\tau(\mathbf{V},\beta) + \frac{\kappa}{1-\nu^2} C(\mathbf{V}(1)) - \bar{\mathcal{B}}_\tau(\beta), \quad (\mathbf{V},\beta) \in H^1(0,1)^2 \times \mathcal{H}_0 \tag{74}$$

where $\tilde{\mathcal{A}}^\kappa_\tau$ *is the restriction of* $\bar{\mathcal{A}}^\kappa_\tau$ *on* $[0,1]$ *and* $C(\mathbf{V}(1)) = \frac{c_{11}}{2} V_1(1)^2 + c_{12} V_1(1) V_2(1) + \frac{c_{22}}{2} V_2(1)^2$ *is defined by*

$$C(\mathbf{V}(1)) = \min_{\mathbf{W} \in \mathbf{H}_{\mathbf{V}(1)}} \tilde{\bar{\mathcal{A}}}^\kappa_\tau(\mathbf{W}), \qquad \mathbf{H}_{\mathbf{V}(1)} = \left\{ W \in H^1(0,\infty)^2 : \mathbf{W}(0) = \mathbf{V}(1) \right\} \tag{75}$$

with

$$\tilde{\bar{\mathcal{A}}}^\kappa_\tau(\mathbf{W}) = \int_0^{+\infty} \left(W_1(\tilde{\zeta})^2 + W_2'(\tilde{\zeta})^2 + 2\nu W_1(\tilde{\zeta}) W_2'(\tilde{\zeta}) + \frac{1-\nu}{2} (W_1'(\tilde{\zeta}) + W_2(\tilde{\zeta}))^2 \right) \mathrm{d}\tilde{\zeta}$$

The study of the positivity of $\mathcal{E}''_t$ *is equivalent to compare the smallest eigenvalue* μ_1 *with zero and* $\mathsf{R}^b_t >$ (resp. $<$)1 *if and only if* $\mu_1 >$ (resp. $<$)0. *The possibility of bifurcation from the fundamental solution is given by*

$$\begin{cases} \mu_1 > 0 & \Longrightarrow \quad \textit{no bifurcation} \\ \mu_1 \leq 0 & \Longrightarrow \quad \textit{bifurcation possible} \end{cases} \tag{76}$$

Moreover, $(\mathbf{V}^{(1)}, \beta^{(1)})$ *is the restriction on* $[0,1]$ *of the first eigenvector of* $\mathcal{E}''_t$.

Proof. Being $\bar{\mathcal{A}}^\kappa_\tau$ and $\bar{\mathcal{B}}_\tau$ positive definite and $\bar{\mathcal{B}}_\tau$ defined on $[0,1]$, the positive definiteness of the quadratic form $\mathcal{E}''_t$ is equivalent to the positive definiteness of

$$\tilde{\mathcal{E}}''_\tau(\mathbf{V},\beta) = \min_{\mathbf{V} \in H^1(1,\infty)^2} \mathcal{E}''_\tau(\mathbf{V},\beta).$$

The expression (74) is obtained by decomposing $\bar{\mathcal{A}}^\kappa_\tau$ in the contributions coming from the integral over $[0,1]$ and $[1,\infty]$. The latter contribution is given by

$$\int_1^\infty \frac{(1-\bar{\alpha}_\tau(\delta_\tau\zeta))^2}{1-\nu^2} \left(\kappa^2 V_1(\zeta)^2 + V_2'(\zeta)^2 + 2\nu\kappa V_1(\zeta) V_2'(\zeta) + \frac{1-\nu}{2} \Big(V_1'(\zeta) + \kappa V_2(\zeta) \Big)^2 \right) \mathrm{d}\zeta \tag{77}$$

which, using the change of variable $\zeta \to 1 + \tilde{\zeta}/\kappa$ and that $\bar{\alpha}_\tau = 0$ in $[1,\infty)$, may be rewritten as $\frac{\kappa}{1-\nu^2} \tilde{\bar{\mathcal{A}}}^\kappa_\tau$.

The criterion for assessing the positivity of the quadratic form $\tilde{\mathcal{E}}''_t$ on the basis of the sign of its smallest eigenvalue is a classical result of the spectral decomposition theorem for a continuous self-joint linear operator on a real Hilbert space and is not discussed further here. □

The quadratic form (74) is a reduced version of the second derivative of the potential energy defined on the finite interval $[0,1]$, instead of on the semi-infinite space $[0,\infty)$. The formulation above is more convenient for the numerical analysis than the Rayleigh ratio bifurcation criterion of Proposition 6 for two main reasons: (i) the availability of efficient numerical methods for the calculation of the smallest eigenvalue of a symmetric matrix; (ii) the formulation of the eigenvalue problem on a finite interval is better suited for the discretization. The effect of the subdomain $[1,\infty]$ is accounted for by an equivalent stiffness localized in $\zeta = 1$ ($C(\mathbf{V}(1))$), which implies a boundary condition of the Robin type in $\zeta = 1$. The coefficients of the quadratic form C are evaluated by solving the linear differential equations obtained as Euler-Lagrange equations for (75). An easy analytical solution is possible for the case $\nu = 0$, giving

$$c_{11} = 2/3 \qquad c_{12} = -1/3 \qquad c_{22} = 2/3.$$

For $\nu \neq 0$ the analytical solution becomes cumbersome and the coefficients must be computed numerically, once for all. The corresponding results obtained through a finite element solver are reported in Figure 8.

They are obtained on a domain long enough to obtain a result almost independent of its length (the solutions of (75) are decaying exponentially with ζ). Note that $c_{11} = c_{22}$.

For the numerical analysis of the sign of (74), we discretize the problem using linear 1d Lagrange finite elements and a uniform mesh. Hence, for given values of the parameters τ, θ, ν and the wave number κ in the x_1-direction, we calculate the smallest eigenvalue $\mu_1(\tau, \kappa, \theta, \nu)$ of the matrix corresponding to the discrete version of (74). The numerical code for this purpose is based on the use of the finite element library `FEniCS` (Logg et al., 2012) and the eigensolvers provided in `SLEPc` (Hernandez et al., 2005).

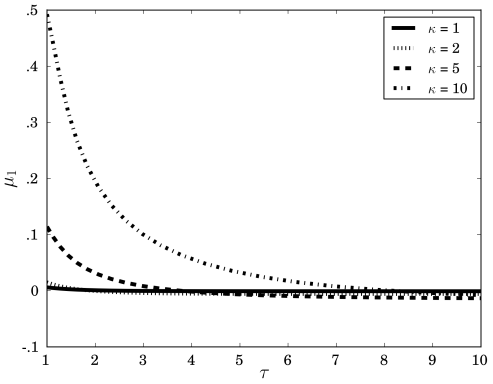

Figure 9: Decreasing of the first eigenvalue μ_1 of the quadratic form (74) with respect to τ for $\theta = .4$, $\nu = 0$ for $\kappa = \{1, 2, 5, 10\}$.

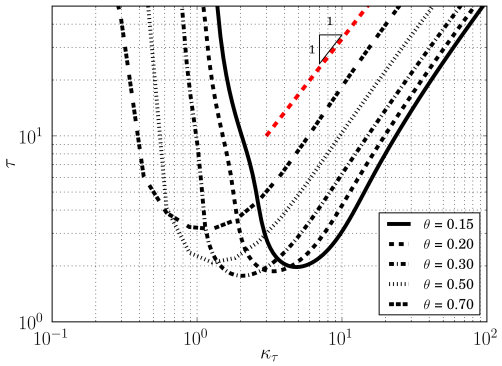

Figure 10: Critical curves separating the states (κ_τ, τ) where the solution of the rate problem is unique and those where bifurcation can occur for different values of the loading parameter θ.

To find the shortest bifurcation time τ_b for which $\mu_1 = 0$ and the associated wave number κ_b we proceed with the following steps:

1. *Initialization.* Set the values of (ν, θ).
2. *Define the critical curve.* Given κ, find $\tau(\kappa)$ such that $\mu_1(\tau, \kappa, \theta, \nu) = 0$, using a bisection algorithm on τ. This gives the *critical curve* in the $\tau - \kappa$ space.
3. *Find the bifurcation point* given by $\kappa_b = \text{argmin}_\kappa \, \mu_1(\tau(\kappa), \kappa, \theta, \nu)$ and $\tau_b = \tau(\kappa_b)$. To this end we use a numerical minimization routine using the downhill simplex algorithm (`fmin` function provided in the optimization toolbox of `SciPy` (Jones et al., 2001–))

For step 2 we are not able to show neither existence nor uniqueness of a solution for the critical τ for a given κ. We found numerically that the $\mu_1(\tau, \kappa, \theta, \nu)$ is a monotonically decreasing function of τ (Fig. 9), which gives us the convergence of the bisection algorithm if a solution exists in the selected initial interval. However, for small values of κ a solution may not exist at all, in agreement with the Property 4 of Proposition 9.

Figure 10 illustrates the critical curves obtained for $\nu = 0$ and different θ. For a given loading θ the critical curve partitions the space (κ, τ) in the region below the curve, where the fundamental solution is the unique solution of the rate problem, and in the region above the curve, where other solutions may exist. During the evolution problem, the first time for which another solution may exist (and indeed it does exist, as stated in Proposition 10), is the minimum point on the critical curve $\kappa \mapsto \tau(\kappa)$. This point is the bifurcation point corresponding to the critical time τ_b and the wave number κ_b (see Proposition 10). The numerical solution provided in Figure 10 may be checked against the qualitative properties of the Rayleigh ratio proved in Proposition 9. Namely, we observe that: (i) the fundamental solution is unique for τ sufficiently small (Properties 1-2); (ii) the fundamental solution is unique for sufficiently small wave numbers even for very long times (Property 4); (iii) for $\kappa \to \infty$, $\tau(\kappa)$ is approximately linear in κ (Property 5).

For the case $\nu = 0$, the critical time τ_b and wave number κ_b at the bifurcation as a function of θ are reported in Figure 11. Figure 12 shows the shape of the damage rate β^b as a function of ζ for the eigenvector associated to the eigenvalue $\mu_1 = 0$.

The key numerical results of this paper are condensed in Figure 13. It shows as a function of θ (and $\nu = 0$) the plots of the critical bifurcation time t_b, wave length $\lambda_b = 2\pi \frac{\theta \delta_{\tau_b} \tau_b}{\kappa_b} \ell$ and penetration of the damage D_b in the physical space and time variables, x_2 and t. The critical time at the bifurcation is reported also as dashed lines in Figure 6, which partitions the $\theta - t$ space in the regions where the fundamental solution is unique or not.

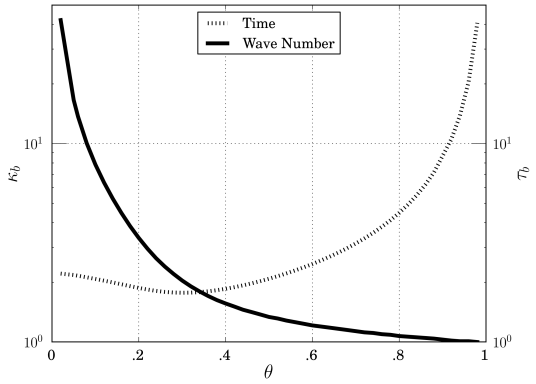

Figure 11: Wave number and rescaled time at the first bifurcation point κ_b, τ_b defined by (57) and (63) for a vanishing Poisson ratio $\nu = 0$.

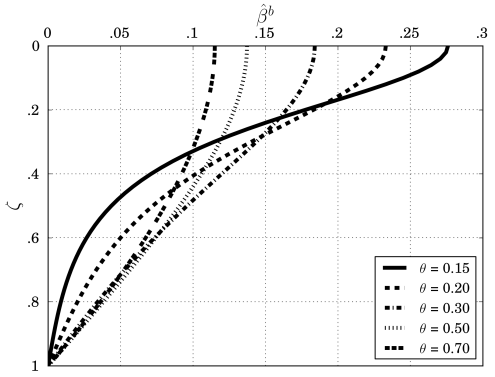

Figure 12: Characterization of damage rate at bifurcation through the eigenvector $\hat{\beta}^b$ (67).

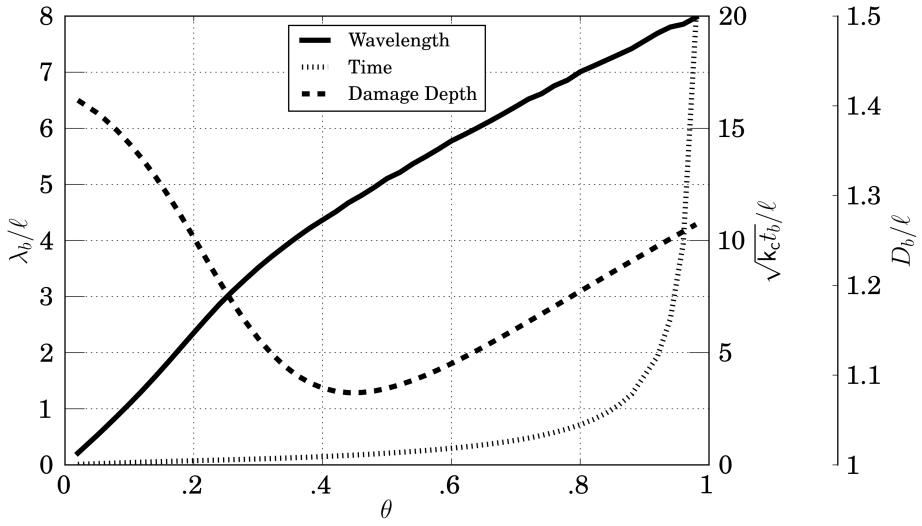

Figure 13: Wavelength λ_b, time t_b and penetration of the damage zone D_b at the first possible bifurcation (given by (65), (68)) for a vanishing Poisson ratio $\nu = 0$ as a function of the loading parameter θ.

Figure 14 shows the influence of the Poisson ratio on the results for a fixed value of θ, showing that the critical wavelength, time and damage depth have a relevant dependence on the Poisson ratio only for ν close to -1. Recall that in plane stress elasticity thermodynamically admissible values of the Poisson ratio are in the interval $(-1, 1)$.

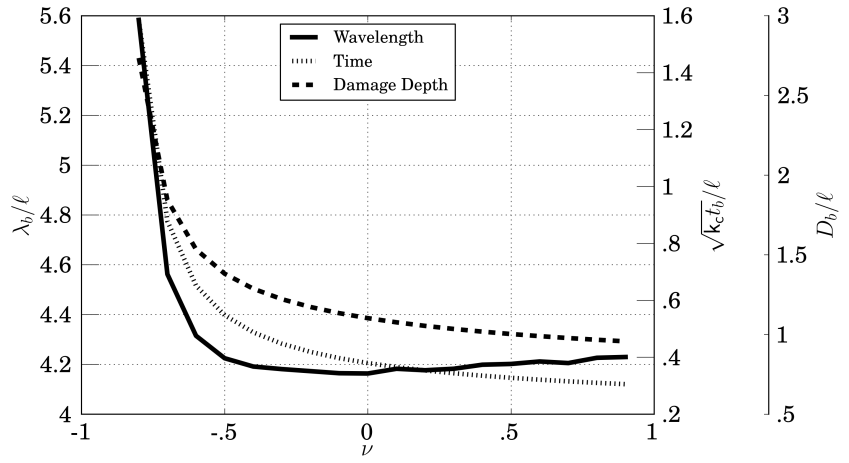

Figure 14: Influence of the Poisson ratio on the characteristic of the first bifurcation point as a function of the loading parameter $\theta = .4$.

6. Comments

6.1. Main results

The analysis of gradient damage models of the previous sections quantitatively predicts the establishment of a fundamental solution with diffuse damage and its bifurcation at a finite time t_b towards a periodic solution. We resume and comment below the main results, coming from our analytical and numerical approaches on a semi-infinite slab.

- *Loading parameter.* The solution of the problem depends on a single dimensionless parameter, the mildness of the thermal shock $\theta = \sigma_c/\mathsf{a}\mathsf{E}\vartheta$, defined as the ratio between the critical stress of the material and the thermal stresses induced by the temperature drop ϑ at the surface, and the Poisson ratio ν. The dependence on the internal length of the damage model ℓ is almost trivial and given explicitly (see below).

- *Existence of a critical severity of the thermal shock.* For mild shocks with $\theta \geq 1$ the solution remains purely elastic at any time and there is not damage at all.

- *Fundamental solution.* If $\theta < 1$ there exists, for any $t > 0$ a solution with diffused damage in a strip, varying monotonically from a maximum damage value $\alpha_t^*(0)$ at the surface to zero at a depth D_t^*. The values of $\alpha_t^*(0)$ and D_t^* as a function of time and the mildness of the thermal shock can be read in Figure 6, where the dashed red line critical time t_b for the first bifurcation toward the periodic solution. This fundamental solution becomes unstable at a finite time $t_s > t_b$ (Proposition 10).

- *Bifurcated solution.* At a finite time t_b there exists a bifurcation from the fundamental solution toward a periodic solution with a wavelength λ_b in the x_1 variable. This bifurcated branch is stable for t sufficiently close to t_b (Proposition 7).

- *Bifurcation time.* The bifurcation time t_b is monotonically increasing with the mildness of the thermal shock. The numerical results of Figure 13 for $\nu = 0$ indicate that it varies from very small values for $\theta \to 0$ to very large values for $\theta \to 1$. Proposition 10 states that t_b is always a strictly positive time.

- *Bifurcation wavelength.* The wavelength of the bifurcated solution is increasing with the mildness of the thermal shock θ. The numerical results of Figure 13 for $\nu = 0$ indicate that it goes to zero for $\theta \to 0^+$. For $\theta \to 1$, it has a finite limit which is of about eight times the internal length, (numerical result for $\theta = .96$).

- *Damage penetration.* The damage penetration at the bifurcation, D_b, is almost independent of the loading (it varies only between ℓ and $1.5\,\ell$), as evident also from Figure 6(b), where the dashed line corresponding to the bifurcation almost coincides with an iso-depth line. Unlike the bifurcation time and wavelength the penetration is non-monotonic with respect to the loading parameter θ. The penetration of the damage band seems to be the parameter triggering the bifurcation and not the maximal value of damage or time which vary with the loading.

- *Influence of the internal length.* The damage penetration in the homogeneous solution D_t and the wavelength λ_b of the bifurcated solution are simply proportional to the internal length ℓ of the damage model. This fact does not really come as surprise, because ℓ is the only characteristic length of the problem for a semi-infinite slab (the characteristic length of the diffusion process associated to the material constant $\mathsf{k_c}$ can be eliminated by a trivial rescaling of the time variable). The bifurcation time t_b is proportional to ℓ^2.

- *Influence of the Poisson ratio.* The fundamental solution is independent of the Poisson ratio. The numerical results of Figure 14 show a weak dependence of the key properties of the bifurcated solution of the Poisson ratio ν, except for $\nu \to -1$.

6.2. From diffuse damage to periodic cracks

The bifurcation toward a periodic solution is the onset of the localization process leading to the formation of periodic crack patterns. The fundamental solution and its bifurcation correspond to the steps 1 and 2 observed in the numerical simulations described in the introduction (see Figure 2). Although the study of the rest of the evolution is outside the scope of the present paper, the numerical experiments show that the oscillations in the damage field further develop by localizing in completely damaged bands. These bands are the regularized representation, typical of gradient damage models, of the periodic array of parallel cracks observed in the experiments. From previous studies in 1d setting (Pham and Marigo, 2013), we know the damage profile in a cross section of each fully developed localization band. In particular, their width L_c and energy dissipated per unit line $\mathsf{G_c}$ (corresponding to the fracture toughness of the cracks) are given by

$$L_c = 2\sqrt{2}\,\ell, \qquad \mathsf{G_c} = \frac{4\sqrt{2}}{3}\frac{{\sigma_\mathsf{c}}^2\ell}{\mathsf{E}}. \tag{78}$$

Most probably, the wavelength λ_b found by the bifurcation analysis is a lower bound on the minimal spacing of the crack at the initiation. Indeed, if the bifurcation is the first step of the localization process into cracks, we have no guarantee that a crack will develop in each period.

The damage model has been introduced using the Young modulus E, the critical stress in a uniaxial tensile test σ_c and the internal length ℓ as material parameters (see Eqns. (1), (10)). Instead of the couple $(\sigma_\mathsf{c}, \ell)$, one can equivalently adopt as independent material constants of the damage model $(\mathsf{G_c}, \sigma_\mathsf{c})$ or $(\mathsf{G_c}, \ell)$ and use (78) for the conversions.

6.3. Domain of applications

In the present paper we made explicit reference to the geometry and loading of the experimental setups for thermal shock on glass or ceramics of Shao et al. (2010, 2011); Bahr et al. (2010); Jiang et al. (2012), where thin specimens of the typical size $50\times10\times1$ mm are heated ($300°C$ - $600°C$) before being dipped into a water bath ($20\ °C$). Thermal shock cracks may appear also in cementitious materials during the exothermic hydration process, where for massive structures the associated temperature drop may reach $40\ °C$. Cracking of the rocks at the wall of gas storage caverns is another example, which is an unwanted consequence of the aggressive operational modes introduced to answer new market regulations. Salt caverns, being initially designed for seasonal storage, *i.e.* a small number of yearly pressure cycles and moderate gas-production rates, are often converted to high-frequency cycling. The rapid release of the gas on a short period of time implies a drop in temperature and a thermal shock for the rocks at the walls of the cavern, where cracks may appear (Berest et al., 2012). The results for thermal loading may be extended by analogy to all the other phenomena governed by a diffusion process which induces a linear shrinkage. The analogy

with drying process of cementitious (Colina and Acker, 2000) or geological (Morris et al., 1992; Chertkov, 2002; Goehring et al., 2009) materials is of particular interest. In this case the temperature field is replaced by the water content or the relative humidity of the material and the thermal shock by a sudden change of the humidity of the environment. In Table 2 we report examples for the relevant material constants for

	E [GPa]	σ_{c} [MPa]	ℓ	$\mathsf{a}\,(\times 10^{-6})$ [K^{-1}]	ϑ	θ
Ceramics	370	270	$50\ \mu m$	8.4	$300 - 600°C$	$0.15 - 0.3$
Gas storage caverns	20	1	$.5 - 2\ m$	40	$30 - 60°C$	$0.02 - 0.04$
Drying of concrete	40	$2 - 3$	$30 - 100\ mm$	$5 - 15$	$40 - 80\, l/m^3$	$0.05 - 0.25$

Table 2: Relevant material parameters and corresponding dimensionless thermal shock mildness parameter θ for ceramics, geomaterials and concrete. The values are purely orientative, giving an indication only of the order of magnitude of the material parameters. The internal length is calculated through equation (78) by using the data available for the critical stress σ_{c} and the fracture toughness G_{c}.

these different situations, giving the corresponding values of the dimensionless parameter appearing in our analysis. The typical order of magnitude of the mildness of the thermal shock θ lies in the range from 0.1 to 0.5. Close settings such as damage induced by solid-solid transformation (Penmecha and Bhattacharya, 2013) are interesting perspectives which could be addressed in the same framework.

7. Conclusion and perspectives

We have studied the initiation of a periodic solution in a gradient damage model under a thermal shock loading. The quasi-static evolution problem for a semi-infinite slab has been formulated in the framework of the variational theory of rate-independent processes. From the first order stability conditions and energy balance, we have proven that, for sufficiently severe thermal shocks, damage initiates at $t = 0$ with non-zero damage diffused in a strip parallel to the surface of the shock. The analysis of the rate problem about this fundamental solution shows the existence of a bifurcation at a finite time t_b towards a stable solution with periodic damage. The fundamental solution becomes unstable at a later time $t_s > t_b$. The bifurcation and stability analysis is based on the study of the sign of the second derivative of the energy in an infinite dimensional setting. The analytical results are obtained by the minimization of a Rayleigh ratio and the decomposition of the solution with a partial Fourier series. Further quantitative results about the time, damage penetration and wavelength at the bifurcation are obtained numerically by solving a one-dimensional eigenvalue problem.

Our work relies on many simplifying hypotheses, which allow us to reach an almost complete analytical treatment of the initiation problem. First, the geometry and the loading are highly idealized. More realistic settings will include the effect of the finite dimension of the slab and a full two-dimensional solution of the thermal problem, eventually accounting for boundary condition of the Robin type on the temperature (Newtonian cooling) and the localized changes in the thermal conductivity due to cracks. The heat boundary condition leads to a maximal value of the stress at the surface at $t = 0$. Boundary conditions on the heat flux could lead to a damage criteria which is not violated at $t = 0$ but would be at a latter time. Three dimensional effects may play a crucial role as soon as the thickness of the slab increases. Further generalization should consider the effect of choice of the damage law, as done in a 1d setting by Pham and Marigo (2013). Here we made a specific choice (see Eqns. (2) and (5)), which assures the existence of a purely elastic response and an easy numerical treatment. An other choice in (5) (e.g. $w(\alpha) = \mathsf{w}\alpha^2$ as in Bourdin et al. (2000) with vanishing stress threshold) would lead to damage nucleation for any loading however small ϑ. We expect that the fundamental mechanism of the creation of the periodic crack pattern as a bifurcation from an x_1-homogenous solution will still apply to a large class softening damage models as those of Pham and Marigo (2013), obviously the numerical results would be different.

The present work is a first attempt to rigorously study the morphogenesis of complex crack patterns in regularized fracture mechanics models. The study of the further localization of the bifurcated solution with periodic damage and of the selective crack propagation typical of the thermal shock problem will be the subject of a further work, currently under preparation. The next step is to compare the semi-analytical

results of this paper to the full scale two-dimensional numerical simulations of Figure 2. The comparison with the experimental results is a further ambitious goal. A key problem is that the distinction between homogeneous damage and periodic fracture is somehow arbitrary, both theoretically and experimentally.

Acknowledgement

J-J. Marigo and C. Maurini gratefully acknowledge the funding of the ANR program T-Shock OTP J11R087.

References

Ambrosio, L., 1990. Existence theory for a new class of variational problems. Archive for Rational Mechanics and Analysis 111 (4), 291–322.
URL http://dx.doi.org/10.1007/BF00376024

Bahr, H. A., Fischer, G., Weiss, H. J., 1986. Thermal-shock crack patterns explained by single and multiple crack propagation. Journal of Materials Science 21, 2716–2720.
URL http://dx.doi.org/10.1007/BF00551478

Bahr, H.-A., Weiss, H.-J., Bahr, U., Hofmann, M., Fischer, G., Lampenscherf, S., Balke, H., 2010. Scaling behavior of thermal shock crack patterns and tunneling cracks driven by cooling or drying. Journal of the Mechanics and Physics of Solids 58 (9), 1411 – 1421.
URL http://dx.doi.org/10.1016/j.jmps.2010.05.005

Bahr, H.-A., Weiss, H.-J., Maschke, H., Meissner, F., 1988. Multiple crack propagation in a strip caused by thermal shock. Theoretical and Applied Fracture Mechanics 10 (3), 219 – 226.
URL http://dx.doi.org/10.1016/0167-8442(88)90014-6

Bazant, Z., Ohtsubo, H., Aoh, K., 1979. Stability and post-critical growth of a system of cooling or shrinkage cracks. International Journal of Fracture 15 (5), 443–456.
URL http://dx.doi.org/10.1007/BF00023331

Benallal, A., Marigo, J.-J., 2007. Bifurcation and stability issues in gradient theories with softening. Modelling and Simulation in Materials Science and Engineering 15 (1), S283.
URL http://stacks.iop.org/0965-0393/15/i=1/a=S22

Berest, P., Djizanne, H., Brouard, B., Hévin, G., 2012. Rapid depressurizations: can they lead to irreversible damage? In: SMRI Spring 2012 Technical Conference.

Bisschop, J., Wittel, F. K., 2011. Contraction gradient induced microcracking in hardened cement paste. Cement and Concrete Composites 33 (4), 466 – 473.
URL http://dx.doi.org/10.1016/j.cemconcomp.2011.02.004

Borden, M. J., Verhoosel, C. V., Scott, M. A., Hughes, T. J., Landis, C. M., 2012. A phase-field description of dynamic brittle fracture. Computer Methods in Applied Mechanics and Engineering 217–220 (0), 77 – 95.
URL http://dx.doi.org/10.1016/j.cma.2012.01.008

Bourdin, B., 2007. The variational formulation of brittle fracture: numerical implementation and extensions. In: Combescure, A and DeBorst, R and Belytschko, T (Ed.), IUTAM Symposium on Discretization Methods for Evolving Discontinuities. Vol. 5 of IUTAM Bookseries. Springer, pp. 381–393.

Bourdin, B., Francfort, G., Marigo, J.-J., 2000. Numerical experiments in revisited brittle fracture. Journal of the Mechanics and Physics of Solids 48 (4), 797 – 826.
URL http://dx.doi.org/10.1016/S0022-5096(99)00028-9

Bourdin, B., Maurini, C., Knepley, M., 2011. Numerical simulation of reservoir stimulation - a variational approach. In: PROCEEDINGS, Thirty-Sixth Workshop on Geothermal Reservoir Engineering Stanford University, Stanford, California, January 31 - February 2, 2011.

Braides, A., 2002. Γ-convergence for beginners. Oxford Lecture Series in Mathematics and its Applications **22**. Oxford University Press, Oxford.

Chertkov, V. Y., 2002. Modelling cracking stages of saturated soils as they dry and shrink. European Journal of Soil Science 53 (1), 105–118.
URL http://dx.doi.org/10.1046/j.1365-2389.2002.00430.x

Colina, H., Acker, P., 2000. Drying cracks: Kinematics and scale laws. Materials and Structures 33, 101–107.
URL http://dx.doi.org/10.1007/BF02484164

Francfort, G., Marigo, J.-J., 1998. Revisiting brittle fracture as an energy minimization problem. Journal of the Mechanics and Physics of Solids 46 (8), 1319 – 1342.
URL http://dx.doi.org/10.1016/S0022-5096(98)00034-9

Gauthier, G., Lazarus, V., Pauchard, L., 2010. Shrinkage star-shaped cracks: Explaining the transition from 90 degrees to 120 degrees. European Physics Letters 89 (2).

Geyer, J. F., Nemat-Nasser, S., 1982. Experimental investigation of thermally induced interacting cracks in brittle solids. International Journal of Solids and Structures 18 (4), 349 – 356.
URL http://dx.doi.org/10.1016/0020-7683(82)90059-2

Goehring, L., Mahadevan, L., Morris, S. W., 2009. Nonequilibrium scale selection mechanism for columnar jointing. Proceedings of the National Academy of Sciences 106 (2), 387–392.
URL http://dx.doi.org/10.1073/pnas.0805132106

Hasselman, D. P. H., 1969. Unified theory of thermal shock fracture initiation and crack propagation in brittle ceramics. Journal of the American Ceramic Society 52 (11), 600–604.
URL http://dx.doi.org/10.1111/j.1151-2916.1969.tb15848.x

Hernandez, V., Roman, J. E., Vidal, V., 2005. SLEPc: A scalable and flexible toolkit for the solution of eigenvalue problems. ACM Transactions on Mathematical Software 31 (3), 351–362.
URL http://www.grycap.upv.es/slepc/

Jagla, E. A., 2002. Stable propagation of an ordered array of cracks during directional drying. Physical Review E 65, 046147.
URL http://link.aps.org/doi/10.1103/PhysRevE.65.046147

Jenkins, D. R., May 2005. Optimal spacing and penetration of cracks in a shrinking slab. Physical Review E 71, 056117.
URL http://link.aps.org/doi/10.1103/PhysRevE.71.056117

Jiang, C., Wu, X., Li, J., Song, F., Shao, Y., Xu, X., Yan, P., 2012. A study of the mechanism of formation and numerical simulations of crack patterns in ceramics subjected to thermal shock. Acta Materialia 60 (11), 4540 – 4550.
URL http://dx.doi.org/10.1016/j.actamat.2012.05.020

Jones, E., Oliphant, T., Peterson, P., et al., 2001–. SciPy: Open source scientific tools for Python.
URL http://www.scipy.org/

Logg, A., Mardal, K.-A., Wells, G. N., et al., 2012. Automated Solution of Differential Equations by the Finite Element Method. Springer.
URL http://dx.doi.org/10.1007/978-3-642-23099-8

Lu, T., Fleck, N., 1998. The thermal shock resistance of solids. Acta Materialia 46 (13), 4755 – 4768.
URL http://dx.doi.org/10.1016/S1359-6454(98)00127-X

Miehe, C., Hofacker, M., Welschinger, F., 2010. A phase field model for rate-independent crack propagation: Robust algorithmic implementation based on operator splits. Computer Methods in Applied Mechanics and Engineering 199 (45 - 48), 2765 – 2778.
URL http://dx.doi.org/10.1016/j.cma.2010.04.011

Morris, P. H., Graham, J., Williams, D. J., 1992. Cracking in drying soils. Canadian Geotechnical Journal 29 (2), 263–277.
URL http://dx.doi.org/10.1139/t92-030

Nguyen, Q., 2000. Stability and Nonlinear Solid Mechanics. Wiley & Son, London.

Nguyen, Q. S., 1994. Bifurcation and stability in dissipative media (plasticity, friction, fracture). Applied Mechanics Reviews 47 (1), 1–31.
URL http://link.aip.org/link/?AMR/47/1/1

Penmecha, B., Bhattacharya, K., 2013. Parallel edge cracks due to a phase transformation. International Journal of Solids and Structures 50 (10), 1550 – 1561.
URL http://dx.doi.org/10.1016/j.ijsolstr.2013.01.027

Pham, K., Marigo, J.-J., 2010a. Approche variationnelle de l'endommagement : I. Les concepts fondamentaux. Comptes Rendus Mécanique 338 (4), 191–198.
URL http://dx.doi.org/10.1016/j.crme.2010.03.009

Pham, K., Marigo, J.-J., 2010b. Approche variationnelle de l'endommagement : II. Les modèles à gradient. Comptes Rendus Mécanique 338 (4), 199–206.
URL http://dx.doi.org/10.1016/j.crme.2010.03.012

Pham, K., Marigo, J.-J., 2013. From the onset of damage to rupture: construction of responses with damage localization for a general class of gradient damage models. Continuum Mechanics and Thermodynamics 25 (2-4), 147–171.
URL http://dx.doi.org/10.1007/s00161-011-0228-3

Pham, K., Marigo, J.-J., Maurini, C., 2011. The issues of the uniqueness and the stability of the homogeneous response in uniaxial tests with gradient damage models. Journal of the Mechanics and Physics of Solids 59 (6), 1163 – 1190.
URL http://dx.doi.org/10.1016/j.jmps.2011.03.010

Shao, Y., Xu, X., Meng, S., Bai, G., Jiang, C., Song, F., 2010. Crack patterns in ceramic plates after quenching. Journal of the American Ceramic Society 93 (10), 3006–3008.
URL http://dx.doi.org/10.1111/j.1551-2916.2010.03971.x

Shao, Y., Zhang, Y., Xu, X., Zhou, Z., Li, W., Liu, B., 2011. Effect of crack pattern on the residual strength of ceramics after quenching. Journal of the American Ceramic Society 94 (9), 2804–2807.
URL http://dx.doi.org/10.1111/j.1551-2916.2011.04728.x

Appendix A. Proof of Proposition 3

Proof. The proof is divided into 8 steps. Throughout the proof τ is a given positive number, $\mathcal{D}_0^1 := \{\beta \in H^1(0,\infty) : 0 \le \beta \le 1\}$ and $\mathcal{D}_0 := \{\beta \in H^1(0,\infty) : 0 \le \beta\}$.

(i) : *Existence and uniqueness of the minimizer.* Since $\bar{\mathcal{E}}_\tau$ is positive and lower semi-continuous and since $\mathcal{D}_0^1$ is closed in $H^1(0,\infty)$, a minimizer exists. Since $\bar{\mathcal{E}}_\tau$ is strictly convex, the minimizer is unique and is denoted by $\bar{\alpha}_\tau$. $\triangleleft$

(ii) : $\bar\alpha_\tau$ *is also the unique minimizer of* $\bar{\mathcal{E}}_\tau$ *over* $\mathcal{D}_0$. By the same arguments as for the minimization over $\mathcal{D}_0^1$, the minimizer exists and is unique, say $\hat\alpha_\tau$. Let us set $\check\alpha_\tau = \min\{\hat\alpha_\tau, 1\} \in \mathcal{D}_0^1 \subset \mathcal{D}_0$. One easily checks that $\bar{\mathcal{E}}_\tau(\check\alpha_\tau) \le \bar{\mathcal{E}}_\tau(\hat\alpha_\tau)$. Therefore $\hat\alpha_\tau = \check\alpha_\tau \in \mathcal{D}_0^1$ and hence $\hat\alpha_\tau = \bar\alpha_\tau$. $\triangleleft$

(iii) : 0 *is not the minimizer.* Since $\theta < 1 = \mathsf{f_c}(0)$, there exists $h > 0$ such that $\theta < \mathsf{f_c}(y)$ in $[0, h]$. Since

$$\bar{\mathcal{E}}'_\tau(0)(\beta) = \int_0^\infty (\theta^2 - \mathsf{f_c}(y)^2)\beta(y)\,\mathrm{d}y,$$

if one chooses $\beta \in \mathcal{D}_0$ with its support included in $[0, h]$, then $\bar{\mathcal{E}}'_\tau(0)(\beta) < 0$ and hence 0 cannot be the minimizer. The (open) support of $\bar\alpha_\tau$ is denoted by I_τ, *i.e.* $I_\tau = \{y \ge 0 : \bar\alpha_\tau(y) > 0\}$. $\triangleleft$

(iv) : $\bar\alpha_\tau$ *is indefinitely continuously differentiable in* I_τ *and satisfies*

$$\frac{1}{\tau^2}\bar\alpha''_\tau(y) + \mathsf{f_c}(y)^2(1 - \bar\alpha_\tau(y)) = \theta^2 \qquad \forall y \in I_\tau. \tag{A.1}$$

Since $\bar\alpha_\tau$ minimizes $\bar{\mathcal{E}}_\tau$ over $\mathcal{D}_0$, by standard arguments one gets that it satisfies

$$\int_0^\infty \left(\frac{1}{\tau^2}\bar\alpha'_\tau(y)\beta'(y) + \Big(\theta^2 - \mathsf{f_c}(y)^2(1 - \bar\alpha_\tau(y))\Big)\beta(y)\right)\mathrm{d}y \ge 0, \quad \forall \beta \in \mathcal{D}_0, \tag{A.2}$$

and the equality holds when $\beta = \bar\alpha_\tau$. Let $\varphi \in C_0^\infty(I_\tau)$ (where $C_0^\infty(I_\tau)$ is the set of indefinitely differentiable functions with compact support in I_τ). For h small enough, $\beta := \bar\alpha_\tau + h\varphi \in \mathcal{D}_0$ and one gets from (A.2)

$$\int_{I_\tau} \left(\frac{1}{\tau^2}\bar\alpha'_\tau(y)\varphi'(y) + \Big(\theta^2 - \mathsf{f_c}(y)^2(1 - \bar\alpha_\tau(y))\Big)\varphi(y)\right)\mathrm{d}y \ge 0.$$

Changing φ in $-\varphi$ gives the opposite sign and the equality for every $\varphi \in C_0^\infty(I_\tau)$. Therefore $\bar\alpha_\tau$ satisfies (A.1) in I_τ. Since $\bar\alpha_\tau$ is continuous and since $\mathsf{f_c}$ is indefinitely continuously differentiable, one deduces by induction that $\bar\alpha_\tau$ is also indefinitely continuously differentiable in I_τ. $\triangleleft$

(v) : *The support* I_τ *is an interval of the form* $[0, \delta_\tau)$ *with* $0 < \delta_\tau \le \infty$. Let us prove by contradiction that there does not exist a connected component (a, b) of I_τ such that $0 < a < b \le \infty$. If such a component exists, then $\bar\alpha_\tau(a) = \bar\alpha_\tau(b) = 0$ (even if $b = \infty$ because $\bar\alpha_\tau$ must tend to 0 at infinity in order to belong to $H^1(0, \infty)$). Let us prove that $\bar\alpha'_\tau(a) = 0$ by using (A.2). For $h > 0$ and small enough, let us consider the family of test functions β_h defined by $\beta_h(y) = 1 - |y - a|/h$ when $|y - a| \le h$ and $\beta_h(y) = 0$ otherwise. Then (A.2) gives

$$0 \le \frac{\alpha_\tau(a - h)}{h} + \frac{\alpha_\tau(a + h)}{h} \le \tau^2 \int_{a-h}^{a+h} \Big(\theta^2 - \mathsf{f_c}(y)^2(1 - \bar\alpha_\tau(y))\Big)\beta_h(y)\,\mathrm{d}y.$$

Passing to the limit when h goes to 0 gives $\bar\alpha'_\tau(a-) = \bar\alpha'_\tau(a+)$ and hence $\bar\alpha_\tau$ is differentiable at a. But since $\bar\alpha_\tau \ge 0$ and $\bar\alpha_\tau(a) = 0$, this is possible if and only if $\bar\alpha'_\tau(a) = 0$. Therefore $\bar\alpha''_\tau(a+)$ must be non negative so that $\bar\alpha_\tau$ be positive in a neighborhood of a. Since $\bar\alpha''_\tau(a+) = \tau^2(\theta^2 - \mathsf{f_c}(a)^2)$ by (A.1), since $\mathsf{f_c}$ is decreasing and since $0 < \bar\alpha_\tau \le 1$ in (a, b), one gets

$$\alpha''_\tau(y) = \tau^2(\theta^2 - \mathsf{f_c}(y)^2(1 - \bar\alpha_\tau(y)) > \tau^2(\theta^2 - \mathsf{f_c}(a)^2) \ge 0, \quad \forall y \in I_\tau.$$

Consequently $\bar\alpha'_\tau$ is increasing and hence positive in I_τ. Hence $\bar\alpha_\tau$ must be increasing in I_τ which is incompatible with $\bar\alpha_\tau(b) = 0$. This is the contradiction and therefore $a = 0$. Consequently, there exists a unique connected component and I_τ is an interval of the form $[0, \delta_\tau)$. $\triangleleft$

(vi) : $\bar\alpha_\tau$ *satisfies the boundary conditions* $\bar\alpha'_\tau(0) = \bar\alpha_\tau(\delta_\tau) = \bar\alpha'_\tau(\delta_\tau) = 0$ *and* δ_τ *is finite.* Taking $\beta = \bar\alpha_\tau$ in (A.2) which is then an equality, integrating by parts the first term in the integral and using (A.1) give $\bar\alpha'_\tau(0)\bar\alpha_\tau(0) = 0$. Since $\bar\alpha_\tau(0) > 0$, one obtains $\bar\alpha'_\tau(0) = 0$. If $\delta_\tau = \infty$, then the boundary conditions at δ_τ are a consequence of $\bar\alpha_\tau$ belongs to $H^1(0, \infty)$ and is indefinitely continuously differentiable. If $\delta_\tau < \infty$, integrating by parts the first term in the integral of (A.2) and using (A.1) leads to

$$\bar\alpha'_\tau(\delta_\tau-)\beta(\delta_\tau) + \tau^2 \int_{\delta_\tau}^\infty (\theta^2 - \mathsf{f_c}(y)^2)\beta(y)\,\mathrm{d}y \ge 0, \quad \forall \beta \in \mathcal{D}_0.$$

This is possible if and only if $\bar{\alpha}'_\tau(\delta_\tau-) \geq 0$ and $\theta \geq \mathsf{f_c}(y)$ for all $y \geq \delta_\tau$. But since $\bar{\alpha}_\tau(\delta_\tau) = 0$ and $\bar{\alpha}_\tau \geq 0$, one also has $\bar{\alpha}'_\tau(\delta_\tau-) \leq 0$. Hence $\bar{\alpha}'_\tau(\delta_\tau-) = 0$ and since $\bar{\alpha}'_\tau(\delta_\tau+) = 0$ one finally has $\bar{\alpha}'_\tau(\delta_\tau) = 0$.

From the inequality $\theta \geq \mathsf{f_c}(y)$ for all $y \geq \delta_\tau$ one deduces that $\delta_\tau \geq \mathsf{f_c}^{-1}(\theta)$. Integrating (A.1) over I_τ gives

$$\theta^2\delta_\tau = \int_0^{\delta_\tau} \mathsf{f_c}(y)^2(1-\bar{\alpha}_\tau(y))\,\mathrm{d}y \leq \int_0^{\infty} \mathsf{f_c}(y)^2\,\mathrm{d}y < \infty$$

and hence δ_τ is finite. $\triangleleft$

(vii) : $\bar{\alpha}_\tau(y)$ *is monotonically decreasing from* $\bar{\alpha}_\tau(0) < 1$ *to 0 when* y *goes from* 0 *to* δ_τ. If $\bar{\alpha}_\tau(0) = 1$, then we should have both $\bar{\alpha}'_\tau(0) = 0$ and $\bar{\alpha}''_\tau(0) = \theta^2 > 0$. Hence $\bar{\alpha}_\tau(y)$ should be greater than 1 for small positive y which is impossible. So, $\bar{\alpha}_\tau(0) < 1$. Let us show that there does not exist a point y where $\bar{\alpha}'_\tau(y) > 0$, by contradiction. If such a point exists, then by continuity there should exist a connected component (a, b) where $\bar{\alpha}'_\tau > 0$. Since $\bar{\alpha}'_\tau(0) = \bar{\alpha}'_\tau(\delta_\tau) = 0$, one should have $\bar{\alpha}'_\tau(a) = \bar{\alpha}'_\tau(b) = 0$. Consequently $\bar{\alpha}''_\tau(a) \geq 0$. But, by (A.1), $\bar{\alpha}''_\tau$ should be increasing in (a, b) (because $\mathsf{f_c}$ and $1-\bar{\alpha}_\tau$ are decreasing). Therefore $\bar{\alpha}''_\tau$ should be positive and hence $\bar{\alpha}'_\tau$ should be increasing in (a, b). That is impossible, hence $\bar{\alpha}'_\tau \leq 0$ everywhere. $\triangleleft$

(viii) : *There exists a unique pair* $(\bar{\alpha}_\tau, \delta_\tau)$ *in* $\mathcal{D}_0 \times (0, +\infty)$ *which satisfies* (38)–(40). Let us first remark that (40) with $\bar{\alpha}_\tau = 0$ in (δ_τ, ∞) implies that

$$\frac{1}{\tau^2}\bar{\alpha}''_\tau(y) + \mathsf{f_c}(y)^2(1-\bar{\alpha}_\tau(y)) \leq \theta^2 \qquad \forall y \in (\delta_\tau, \infty). \tag{A.3}$$

Multiplying (38) and (A.3) by $\beta \in \mathcal{D}_0$, integrating over $(0, \delta_\tau) \cup (\delta_\tau, \infty)$, integrating by parts and using (39) leads to (A.2). Moreover the equality holds when $\beta = \bar{\alpha}_\tau$. Therefore $\bar{\alpha}_\tau \in \mathcal{D}_0$ is such that $\bar{\mathcal{E}}'_\tau(\bar{\alpha}_\tau)(\beta - \bar{\alpha}_\tau) \geq 0$ for all $\beta \in \mathcal{D}_0$ which is a characterization of the unique minimizer of $\bar{\mathcal{E}}_\tau$ over $\mathcal{D}_0$. $\triangleleft$ $\square$

Appendix B. Proof of Proposition 7

Proof. $\|\cdot\|$ denotes indiscriminately the natural norm on $H^1(\Omega)$ and $H^1(\Omega)^2$. Let $s \in (t, t+\eta)$, $(\mathbf{v}, \beta) \in \mathcal{C} \times \dot{\mathcal{D}}_s^+$, $(\mathbf{v}, \beta) \neq (0, 0)$ and let h be a small positive real number. Expanding with respect to h up to the second order gives

$$\mathcal{E}_t(\mathbf{u}_s + h\mathbf{v}, \alpha_s + h\beta) = \mathcal{E}_s(\mathbf{u}_s, \alpha_s) + \mathcal{E}'_s(\mathbf{u}_s, \alpha_s)(\mathbf{v}, \beta) + \frac{1}{2}\mathcal{E}''_s(\mathbf{u}_s, \alpha_s)(\mathbf{v}, \beta) + \wr(h)$$

Since the evolution is stationary we have $\mathcal{E}'_t(\mathbf{u}_s, \alpha_s)(\mathbf{v}, \beta) \geq 0$. Thus it is sufficient to prove $\mathcal{E}''_t(\mathbf{u}_s, \alpha_s)(\mathbf{v}, \beta) > 0$ for proving the stability of $(\mathbf{u}_s, \alpha_s)$ in the direction $(\mathbf{v}, \beta)$. By continuity the quadratic form $\mathcal{E}''_t(\mathbf{u}_s, \alpha_s)$ converges to the quadratic form $\mathcal{E}''_t(\mathbf{u}_t, \alpha_t)$ when s tends to t and

$$\forall (\mathbf{v}, \beta) \in \mathcal{C} \times H^1(\Omega) \qquad |\left(\mathcal{E}''_s(\mathbf{u}_s, \alpha_s) - \mathcal{E}''_t(\mathbf{u}^*_t, \alpha^*_t)\right)(\mathbf{v}, \beta)| \leq \mathcal{O}(s-t)(\|\mathbf{v}\|^2 + \|\beta\|^2)$$

where $\mathcal{O}(\cdot)$ is bounded on $[0, \eta)$ and $\lim_{\varsigma \to 0} \mathcal{O}(\varsigma) = 0$. Therefore it is sufficient to prove that there exist C_t such that

$$\forall (\mathbf{v}, \beta) \in \mathcal{C} \times \dot{\mathcal{D}}_t^+ \qquad \mathcal{E}''_t(\mathbf{u}^*_t, \alpha^*_t)(\mathbf{v}, \beta) \geq C_t(\|\mathbf{v}\|^2 + \|\beta\|^2) \tag{B.1}$$

Indeed, in such a case for η sufficiently small we will have for all $s \in (t, t+\eta)$

$$\mathcal{E}''_s(\mathbf{u}_s, \alpha_s)(\mathbf{v}, \beta) \geq (C_t - \mathcal{O}(s-t))(\|\mathbf{v}\|^2 + \|\beta\|^2) > 0$$

Since $t < t_s$ the state $(\mathbf{u}^*_t, \alpha^*_t)$ is stable and $\mathsf{R}^s_t = \min_{\mathcal{C} \times \dot{\mathcal{D}}_t^+} \mathcal{R}^*_t > 1$. By definition of see (53) we have

$$\forall (v, \beta) \in \mathcal{C} \times \dot{\mathcal{D}}_t^+ \qquad \mathcal{E}''_t(\mathbf{u}^*_t, \alpha^*_t)(\mathbf{v}, \beta) \geq \left(1 - \frac{1}{\mathsf{R}^s_t}\right)\mathcal{A}^*_t(\mathbf{v}, \beta) \geq 0$$

with the equality to 0 if and only if $(\mathbf{v}, \beta) = (0, 0)$. Thus we obtain (B.1). $\square$

Appendix C. Proof of Proposition 5

Proof. The three items (IR), (ST) and (EB) give the following necessary conditions for $(\dot{\mathbf{u}}, \dot{\alpha})$:

1. By (IR), we get $\dot{\alpha} \geq 0$ and hence $(\dot{\mathbf{u}}, \dot{\alpha}) \in \mathcal{C} \times \mathcal{D}_+$;
2. The stability condition (ST) implies the first order stability conditions which at time $t+h$ read as

$$\forall (\mathbf{v}, \beta) \in \mathcal{C} \times \mathcal{D}_+, \qquad \mathcal{E}'_{t+h}(\mathbf{u}_{t+h}, \alpha_{t+h})(\mathbf{v}, \beta) \geq 0. \tag{C.1}$$

   Let us discriminate between two types of direction:
   (a) For the directions $(\mathbf{v}, \beta)$ such that $\mathcal{E}'_t(\mathbf{u}^*_t, \alpha^*_t)(\mathbf{v}, \beta) > 0$, by continuity the inequality (C.1) holds for h small enough and hence (ST) is satisfied.
   (b) Considering the directions $(\mathbf{v}, \beta)$ such that $\mathcal{E}'_t(\mathbf{u}^*_t, \alpha^*_t)(\mathbf{v}, \beta) = 0$. By virtue of (26)-(27) they correspond to the directions such that $\beta = 0$ in the undamaged domain at time t $\Omega^e_t = \Omega \setminus \Omega^d_t$. Dividing the inequality (C.1) by h and passing to the limit when h goes to 0 give the following inequality that the $(\dot{\mathbf{u}}, \dot{\alpha})$ rate must satisfy

$$\forall (\mathbf{v}, \beta) \in \mathcal{C} \times \mathcal{D}_+ \quad \mathcal{E}''_t(\mathbf{u}^*_t, \alpha^*_t) \langle (\dot{\mathbf{u}}, \dot{\alpha}), (\mathbf{v}, \beta) \rangle + \dot{\mathcal{E}}'_t(\mathbf{u}^*_t, \alpha^*_t)(\mathbf{v}, \beta) \geq 0. \tag{C.2}$$

   In (C.2), $\mathcal{E}''_t(\mathbf{u}^*_t, \alpha^*_t)$ represents the symmetric bilinear form associated with the quadratic form defined in (20), while $\dot{\mathcal{E}}'_t(\mathbf{u}^*_t, \alpha^*_t)$ is the linear form given by (21).
3. We deduce from the Kuhn-Tucker conditions in the bulk at time t, see Proposition 2, that $\dot{\alpha} = 0$ in Ω^e_t. The energy balance (EB) reads at time $t+h$

$$\begin{aligned} 0 &= \mathcal{E}_{t+h}(\boldsymbol{\chi}_{t+h}) - \mathcal{E}_t(\boldsymbol{\chi}^*_t) + \int_t^{t+h} \int_\Omega \boldsymbol{\sigma}_s \cdot \dot{\boldsymbol{\varepsilon}}^{\mathrm{th}}_s \, \mathrm{d}\mathbf{x} \, \mathrm{d}s \\ &= \mathcal{E}_{t+h}(\boldsymbol{\chi}_{t+h}) - \mathcal{E}_{t+h}(\boldsymbol{\chi}^*_t) + \mathcal{E}_{t+h}(\boldsymbol{\chi}^*_t) - \mathcal{E}_t(\boldsymbol{\chi}^*_t) + \int_t^{t+h} \int_\Omega \boldsymbol{\sigma}_s \cdot \dot{\boldsymbol{\varepsilon}}^{\mathrm{th}}_s \, \mathrm{d}\mathbf{x} \, \mathrm{d}s \end{aligned} \tag{C.3}$$

   where $\boldsymbol{\sigma}_s = (1-\alpha_s)^2 \mathbf{A}(\boldsymbol{\varepsilon}(\mathbf{u}_s) - \boldsymbol{\varepsilon}^{\mathrm{th}}_s)$, $\boldsymbol{\chi}_{t+h} = (\mathbf{u}_{t+h}, \alpha_{t+h})$ and $\boldsymbol{\chi}^*_t = (\mathbf{u}^*_t, \alpha^*_t)$. A first expansion of (C.3) gives

$$\begin{aligned} 0 &= \mathcal{E}'_{t+h}(\boldsymbol{\chi}^*_t)(\boldsymbol{\chi}_{t+h} - \boldsymbol{\chi}^*_t) + \frac{1}{2}\mathcal{E}''_{t+h}(\boldsymbol{\chi}^*_t)(\boldsymbol{\chi}_{t+h} - \boldsymbol{\chi}^*_t) + \mathcal{E}_{t+h}(\boldsymbol{\chi}^*_t) - \mathcal{E}_t(\boldsymbol{\chi}^*_t) \\ &\quad + \int_t^{t+h} \int_\Omega \boldsymbol{\sigma}_s \cdot \dot{\boldsymbol{\varepsilon}}^{\mathrm{th}}_s \, \mathrm{d}\mathbf{x} \, \mathrm{d}s + o(\|\boldsymbol{\chi}_{t+h} - \boldsymbol{\chi}^*_t\|^2) \end{aligned} \tag{C.4}$$

   where $\mathcal{E}''_t(\boldsymbol{\chi}^*_t)$ is the quadratic form defined in (20), $\|\cdot\|$ denotes the natural norm on $\mathcal{C} \times \mathcal{D}$. A second expansion leads to

$$\begin{aligned} 0 &= \mathcal{E}'_t(\boldsymbol{\chi}^*_t)(\boldsymbol{\chi}_{t+h} - \boldsymbol{\chi}^*_t) + h^2 \dot{\mathcal{E}}'_t(\boldsymbol{\chi}^*_t)(\dot{\boldsymbol{\chi}}) + \frac{h^2}{2}\mathcal{E}''_t(\boldsymbol{\chi}^*_t)(\dot{\boldsymbol{\chi}}) + h\dot{\mathcal{E}}_t(\boldsymbol{\chi}^*_t) + \frac{h^2}{2}\ddot{\mathcal{E}}_t(\boldsymbol{\chi}^*_t) \\ &\quad + h\int_\Omega \boldsymbol{\sigma}^*_t \cdot \dot{\boldsymbol{\varepsilon}}^{\mathrm{th}}_t \, \mathrm{d}\mathbf{x} + \frac{h^2}{2}\int_\Omega (\boldsymbol{\sigma}^*_t \cdot \ddot{\boldsymbol{\varepsilon}}^{\mathrm{th}}_t + \dot{\boldsymbol{\sigma}}^*_t \cdot \dot{\boldsymbol{\varepsilon}}^{\mathrm{th}}_t) \, \mathrm{d}\mathbf{x} + o(h^2) \end{aligned} \tag{C.5}$$

   where $\dot{\boldsymbol{\chi}} = (\dot{\mathbf{u}}, \dot{\alpha})$ and $\dot{\boldsymbol{\sigma}}$ is the right derivative of $t \mapsto \boldsymbol{\sigma}_t$ at t. Let us examine the different terms of (C.5):
   (a) Using (6), (25), (26), (35)–(39), one gets

$$\mathcal{E}'_t(\boldsymbol{\chi}^*_t)(\boldsymbol{\chi}_{t+h} - \boldsymbol{\chi}^*_t) = \int_{\Omega^d_{t+h} \setminus \Omega^d_t} \left(\mathsf{w} - \mathsf{Ea}^2 \vartheta^2 \, {\mathsf{f_c}}^2 \left(\frac{x_2}{2\sqrt{\mathsf{k_c} t}} \right) \right) \alpha_{t+h}(\mathbf{x}) \, \mathrm{d}\mathbf{x}.$$

   By virtue of Hypotheses 1 and 3, α_{t+h} is continuously differentiable and vanishes outside Ω^d_t. Therefore $\max_{\Omega^d_{t+h} \setminus \Omega^d_t} |\alpha_{t+h}| = o(h)$ since $\Omega^d_{t+h} \setminus \Omega^d_t$ is included in a strip of width Ch. Hence $\mathcal{E}'_t(\boldsymbol{\chi}^*_t)(\boldsymbol{\chi}_{t+h} - \boldsymbol{\chi}^*_t) = o(h^2)$ (in the case of the fundamental branch, this term is of the order of h^3);

(b) By virtue of (17), $\dot{\mathcal{E}}_t(\boldsymbol{\chi}_t^*) = -\int_\Omega \boldsymbol{\sigma}_t^* \cdot \dot{\boldsymbol{\varepsilon}}_t^{\rm th}\,\mathrm{d}\mathbf{x}$;
(c) By virtue of (18), $\ddot{\mathcal{E}}_t(\boldsymbol{\chi}_t^*) = \int_\Omega((1-\alpha_t^*)^2\mathbf{A}\dot{\boldsymbol{\varepsilon}}_t^{\rm th}\cdot\dot{\boldsymbol{\varepsilon}}_t^{\rm th} - \boldsymbol{\sigma}_t^*\cdot\ddot{\boldsymbol{\varepsilon}}_t^{\rm th})\,\mathrm{d}\mathbf{x}$.

Using all these calculations, dividing (C.5) by h^2 and passing to the limit when h goes to 0, one finally obtains

$$\mathcal{E}_t''(\boldsymbol{\chi}_t^*)(\dot{\boldsymbol{\chi}}) + \dot{\mathcal{E}}_t'(\boldsymbol{\chi}_t^*)(\dot{\boldsymbol{\chi}}) = 0. \tag{C.6}$$

where by virtue of (21), $\dot{\mathcal{E}}_t'(\boldsymbol{\chi}_t^*)(\dot{\boldsymbol{\chi}}) = -\int_\Omega(\dot{\boldsymbol{\sigma}}\cdot\dot{\boldsymbol{\varepsilon}}_t^{\rm th} + (1-\alpha_t^*)^2\mathbf{A}\dot{\boldsymbol{\varepsilon}}_t^{\rm th}\cdot\dot{\boldsymbol{\varepsilon}}_t^{\rm th})\,\mathrm{d}\mathbf{x}$.

Equation (47) is a direct consequence of (C.2) and (C.6). □

Appendix D. Proof of Proposition 9

Proof. Throughout the proof we use the notations of Section 4.3.

1. By virtue of the positivity of the sum of the first two terms in the right hand side of (61) and since $\mathsf{f_c} \le 1$ everywhere, one gets

$$\bar{\mathcal{R}}_\tau^\kappa(\mathbf{V},\beta) \ge \frac{1}{3\delta_\tau^2\tau^2}\frac{\int_0^1 \beta'^2\,\mathrm{d}\zeta}{\int_0^1\beta^2\,\mathrm{d}\zeta}, \quad \forall\,\mathbf{V}\in\mathbf{H}, \quad \forall\beta\in\mathcal{H}_0\setminus\{0\}$$

and hence

$$\min_{\mathbf{H}\times\mathcal{H}_0}\bar{\mathcal{R}}_\tau^\kappa \ge \frac{1}{3\delta_\tau^2\tau^2}\min_{\beta\in\mathcal{H}_0\setminus\{0\}}\frac{\int_0^1\beta'^2\,\mathrm{d}\zeta}{\int_0^1\beta^2\,\mathrm{d}\zeta} = \frac{\pi^2}{12\delta_\tau^2\tau^2}.$$

Since, by Proposition 4, δ_τ varies continuously from δ_0 to δ_∞, $\max_\tau\delta_\tau<\infty$ and the result follows.

2. It is a direct consequence of the previous estimate, of the definition (63) of τ and of the definition (60) of R_t^b.

3. Let us consider the following pair $(\mathbf{v},\beta)$ in $\mathcal{C}\times\dot{\mathcal{D}}_t^+$:

$$\beta(\mathbf{x}) = \check{\beta}(\zeta)\Big(1+\cos(k\pi\frac{x_1}{\mathsf{L}})\Big), \qquad \mathbf{v}(\mathbf{x}) = 2\mathsf{a}\vartheta\delta_\tau\sqrt{\mathsf{k_c}t}\,\check{V}(\zeta)\sin(k\pi\frac{x_1}{\mathsf{L}})\mathbf{e}_1,$$

where $\check{\beta}\in\mathcal{H}_0\cap\{\beta\ge 0\}$, $\check{V}\in H^1(0,\infty)$ and $k\in\mathbb{N}_*$. Inserting into (53) and using (61)–(62) give

$$\mathsf{R}_t^s \le \mathcal{R}_t^*(\mathbf{v},\beta) = \frac{2\bar{\mathcal{A}}_\tau^0(\mathbf{0},\check{\beta}) + \bar{\mathcal{A}}_\tau^\kappa(\check{V}\mathbf{e}_1,\check{\beta})}{3\bar{\mathcal{B}}_\tau(\check{\beta})}.$$

After some calculations, one gets $3\bar{\mathcal{B}}_\tau(\check{\beta}) = 9\int_0^1\mathsf{f_c}(\delta_\tau\zeta)^2\check{\beta}(\zeta)^2\,\mathrm{d}\zeta$ and

$$\begin{aligned}
2\bar{\mathcal{A}}_\tau^0(\mathbf{0},\check{\beta}) + \bar{\mathcal{A}}_\tau^\kappa(\check{V}\mathbf{e}_1,\check{\beta}) \;=\; & \int_0^\infty(1-\bar\alpha_\tau(\delta_\tau\zeta))^2\left(\frac{\kappa^2\check{V}(\zeta)^2}{1-\nu^2}+\frac{\check{V}'(\zeta)^2}{2(1+\nu)}\right)\mathrm{d}\zeta\\
& + \int_0^1\Big(-4(1-\bar\alpha_\tau(\delta_\tau\zeta))\mathsf{f_c}(\delta_\tau\zeta)\kappa\check{V}(\zeta)\check{\beta}(\zeta) + 12\mathsf{f_c}(\delta_\tau\zeta)^2\check{\beta}(\zeta)^2\Big)\mathrm{d}\zeta\\
& + \frac{1}{\delta_\tau^2\tau^2}\int_0^1\Big(\kappa^2\check{\beta}(\zeta)^2 + 3\check{\beta}'(\zeta)^2\Big)\mathrm{d}\zeta.
\end{aligned}$$

Taking

$$\check{V}(\zeta) = \frac{1-\nu^2}{\kappa}\frac{\mathsf{f_c}(\delta_\tau\zeta)}{1-\bar\alpha_\tau(\delta_\tau\zeta)}\check{\beta}(\zeta)$$

and passing to the limit when $t\to\infty$ yields

$$\lim_{t\to\infty}\mathsf{R}_t^s \le \frac{8-4\nu^2}{9} + \frac{C(\check{\beta})}{\kappa^2},$$

where $C(\check{\beta})$ depends on $\check{\beta}$ but not on κ. Passing to the limit when κ goes to ∞ gives the desired inequality for R_t^s. Since $\mathsf{R}_t^b\le\mathsf{R}_t^s$ (Remark 1) the result follows.

4. When $\kappa = 0$, the crossed term of β with $\mathbf{V}$ vanishes in $\bar{\mathcal{R}}_\tau^\kappa(\mathbf{V}, \beta)$. Therefore, $\mathbf{V} = \mathbf{0}$ is the minimizer of $\mathcal{R}_\tau^0$ at every $\tau > 0$. Accordingly, one gets

$$\min_{\mathbf{H}\times\mathcal{H}_0} \mathcal{R}_\tau^0 = \frac{4}{3} + \frac{1}{3\delta_\tau^2\tau^2} \min_{\beta\in\mathcal{H}_0\setminus\{0\}} \frac{\int_0^1 \beta'(\zeta)^2 \,\mathrm{d}\zeta}{\int_0^1 \mathsf{f_c}(\delta_\tau\zeta)^2\beta(\zeta)^2 \,\mathrm{d}\zeta},$$

from which one easily deduces the announced property.

5. The behavior of $\min_{\mathbf{H}\times\mathcal{H}_0} \bar{\mathcal{R}}_\tau^\kappa$ when κ goes to infinity is a problem of singular perturbation in which the sequence of minimizers degenerates. So, this asymptotic behavior is obtained by a direct approach. First, one deduces from (61)-(62) the following estimate:

$$\bar{\mathcal{R}}_\tau^\kappa(\mathbf{V}, \beta) \geq \frac{\kappa^2}{3\delta_\tau^2\tau^2} \frac{\int_0^1 \beta(\zeta)^2 \,\mathrm{d}\zeta}{\int_0^1 \mathsf{f_c}(\delta_\tau\zeta)^2\beta(\zeta)^2 \,\mathrm{d}\zeta} > \frac{\kappa^2}{3\delta_\tau^2\tau^2}, \qquad \forall\,(\mathbf{V}, \beta) \in \mathbf{H}\times(\mathcal{H}_0 \setminus \{0\}),$$

where the second inequality is due to $\mathsf{f_c} < 1$ in $(0, 1)$. Therefore one obtains the following lower bound for the limit of the minimum when $\kappa \to \infty$:

$$\lim_{\kappa\to\infty} \frac{\min_{\mathbf{H}\times\mathcal{H}_0} \bar{\mathcal{R}}_\tau^\kappa}{\kappa^2} \geq \frac{1}{3\delta_\tau^2\tau^2}.$$

It remains to construct a minimizing sequence such that the equality holds at the limit. Let β^κ be the sequence defined by $\beta^\kappa(\zeta) = \max\{1 - \kappa\zeta, 0\}$. Hence $\beta^\kappa \in \mathcal{H}_0$ and $\bar{\mathcal{R}}_\tau^\kappa(\mathbf{0}, \beta^\kappa)/\kappa^2$ is given by

$$\frac{\bar{\mathcal{R}}_\tau^\kappa(\mathbf{0}, \beta^\kappa)}{\kappa^2} = \frac{1}{3\delta_\tau^2\tau^2} \frac{\int_0^{1/\kappa} (1 - \kappa\zeta)^2 \,\mathrm{d}\zeta + 1/\kappa}{\int_0^{1/\kappa} \mathsf{f_c}(\delta_\tau\zeta)(1 - \kappa\zeta)^2 \,\mathrm{d}\zeta} + \frac{4}{3\kappa^2}$$

and passing to the limit yields

$$\lim_{\kappa\to\infty} \frac{\bar{\mathcal{R}}_\tau^\kappa(\mathbf{0}, \beta^\kappa)}{\kappa^2} = \frac{1}{3\delta_\tau^2\tau^2}.$$

The proof is complete. □